

## Supplementary Material

### *Vectipelta barretti*, a new ankylosaur from the Lower Cretaceous Wessex Formation of the Isle of Wight, UK

Stuart Pond\*<sup>1</sup>, Sarah-Jane Strachan<sup>2</sup>, Thomas J. Raven<sup>1</sup>, Martin I. Simpson<sup>3</sup>, Kirsty Morgan<sup>4</sup> and Susannah C.

R. Maidment\*<sup>1</sup>

1. Fossil Reptiles, Amphibians and Birds Section, Natural History Museum, Cromwell Road, London SW7 5BD, United Kingdom.
2. Department of Earth Sciences, University College London, Gower Street, London, WC1E 6BT.
3. Lansdowne, Military Road, Chale, Isle of Wight, PO38 2HH, United Kingdom.
4. Fayetteville, Arkansas, 72701, United States.

\*Corresponding authors: [s.pond@nhm.ac.uk](mailto:s.pond@nhm.ac.uk); [susannah.maidment@nhm.ac.uk](mailto:susannah.maidment@nhm.ac.uk)

#### Methods

The holotype of *Vectipelta barretti*, IWCMS:2020:153 and IWCMS 2021.75, was recorded using manual photogrammetry, an established and widely-used technique (Mallison and Wings 2014) for creating 3D point clouds and meshes by taking overlapping photographs of a subject that are then processed using specialist software. Photogrammetry is capable of recording detail to sub-millimetre resolution with a high degree of reproducibility (Fahlke and Autenrieth 2016), with an accuracy superior to that of a hand scanner (Díez Díaz et al. 2021).

Photographs were taken on a Fuji X10 camera mounted on a tripod. To minimise depth of field F-stops were set between f8-f12 and ISO was kept as low as possible to avoid noise artefacts, and adjusted according to ambient light conditions and specimen colour.

Specimens to be photographed were placed on a small turntable located in an open-topped, portable photobooth 50cmx50cmx50cm with white fabric sides that allow the diffusion of the lights that are positioned on either side. A light with a diffuse filter was positioned above the turntable and two lights were also positioned either side of the booth to fill any shadows on the specimen. A fourth light with a diffuse filter was attached to the tripod and positioned slightly behind and to the left of the camera to fill any shadows on the underside of the specimen. All images were shot with the camera's built-in flash to further eliminate shadows and were bracketed if required. Shooting took place mostly during daylight hours with a large window situated to the right of the photobooth providing natural light and with the room lights on to maximise ambient light.

The turntable was marked in 20° increments and specimens were shot in three passes, each at a different height,

with the turntable being rotated in 10° or 20° increments until a series of overlapping photographs resulting in 360° coverage of the subject at each height. For some specimens an additional set of photographs were taken from directly above the specimen using the camera handheld. The subject was then reorientated and repositioned, and the process repeated until the entire surface of the subject had been recorded.

Images were saved as RAW files or JPEGs that were then batch converted into TIFF files using Adobe Photoshop, which allows alpha channels to be saved in each file alongside the image data. Levels were corrected for each photograph individually and the subject isolated by hand using the 'Quick Selection', 'Magic Wand' 'Select > subject' and 'Brush' tools. An alpha channel was then generated from this selection and saved using a custom Photoshop action, creating a mask that isolates the subject of each photograph from the background.

The TIFF files for each specimen, including mask data, were loaded into Agisoft Photoscan Standard (various build numbers) and Metashape (various build numbers), which were then used to generate single-chunk 3D point clouds, 3D meshes and textures following the methods described in Mallison and Wings, 2014. Meshes were exported as OBJ files and textures as JPEGs.

Meshes were then imported into Cinema 4D R16 and R21 for scaling and reorientation to facilitate digital reconstruction and allow figures to be created. For figures, two versions of each specimen were rendered. The first set of renders are of the model with the original texture intact, essentially creating an image virtually indistinguishable from a photograph. A second set of images was then rendered used a digital version of the palaeontological technique of smoking specimens to coat them with ammonium chloride to enhance surface detail prior to photography (Shelburne and Thompson 2016). A matt white texture was created that reduces reflectivity to eliminate specular highlights, and this replaced the original texture of the 3D mesh. These 3D meshes were then lit using multiple lights to eliminate deep shadows and blowout of lighter areas of the texture. Ambient Occlusion was turned on during rendering at 100% accuracy with minimum samples set to 20 and maximum samples set to 200, to enhance the rendering of shadows to emphasise fine surface detail.

3D skeletal reconstruction was carried out using Cinema 4D and zBrush. Complete individual bones that were part of the specimen are represented by the mesh generated by photogrammetry and were imported as OBJ files into Cinema 4D. Where required, the retopologising of meshes generated by photogrammetry was carried out in zBrush using the zRemesher function.

Bones missing from the specimen were initially modelled in Maxon Cinema 4D using the technique of polygon modelling. This base mesh was then saved as an .obj file and the base and guide meshes (if used) imported into zBrush, a 3D sculpting application which allows the manipulation of 3D data in a manner that simulates working with clay and that is well suited to sculpting organic shapes. The form of each bone was refined, and any detail added. Partial and missing bones were modelled using reference material drawn from the literature, specimen photographs and measurements taken from specimens observed first-hand by the authors or obtained and using data from photogrammetry of the bones of the holotype of *Polacanthus foxi* NHMUK PV R175 and a generic skeletal reconstruction of *Edmontonia* created by SBP (Sellers and Pond 2015).

The final individual bone meshes were then exported from zBrush as Wavefront Object files and these reimported into Cinema 4D to be assembled into a whole skeleton in a neutral standing pose. The assembled 3D skeleton was then used as the basis of a traditional 2D black and white reconstruction as well as 3D life restoration. The skull sculpt was based on CT data of *Panoplosaurus mirus* (Witmer and Ridgely, 2008). Myological reconstruction was completed with reference to Coombs (1979), Hartman (pers. comm.), Brusatte (2012), and Witton (2018). Manus configuration was informed by Senter (2010).

## Synapomorphies

The below synapomorphies show the transition of character states for a given character, by either ambiguous (-->) or unambiguous (==>) transitions.

The clade containing *Vectipelta*, *Dongyangopelta* and *Zhejiangosaurus* (node 134 -> 133) is supported by:

- Character 132 - Cervical vertebrae, anterior and posterior facets of centra: aligned (0), anterior facet dorsal to posterior facet (1), anterior facet ventral to posterior facet (2). 0 --> 1
- Character 156 - Sacral rod vertebrae (i.e. dorsal vertebrae fused to the sacrum), number: zero (0), one (1), two (2), three (3), four (4), five or more (5). 3 ==> 5
- Character 179 - Middle and posterior caudal vertebrae, longitudinal ridge at approximate mid-height of centrum: absent (0), present (1). 0 ==> 1
- Character 200 - Humerus, separation of humeral head and deltopectoral crest in anterior view: continuous (0), separated by a distinct notch (1). 0 --> 1
- Character 246 - Ischium, posterior end of ischium: expanded relative to the shaft (0), not expanded (1), tapers posteriorly (2). 1 --> 0
- Character 257 - Tibia, maximum distal width compared to the maximum proximal width: narrower (0), wider (1). 1 --> 0
- Character 330 - Form of pelvic (sacral) osteoderms: unfused (0), co-ossified osteoderm rosettes (1), co-ossified evenly-sized polygons (2). 2 ==> 1

The clade (above) containing *Vectipelta* is itself sister taxon to a clade containing a large number of 'ankylosaurid' ankylosaurs, including *Shamosaurus*, *Zaraapelta*, *Euoplocephalus*, *Saichania*, *Jinyunpelta* and *Ankylosaurus*, among others. The sister-taxon relationship (Node 149 -> 135) between the two clades is supported by:

- Character 2 - Lateral temporal fenestra: present (0), absent (1). 0 --> 1
- Character 7 - Posterior margin of the skull, transverse width (including squamosal osteoderms where applicable) relative to the maximum width across the orbits (i.e. the lateral margins of the skull at this point): greater (0), equal (1), less (2). 2 ==> 0
- Character 34 - External nares, in dorsal view: visible (0), not visible (1). 0 --> 1
- Character 52 - Lacrimal, long axis of main body orientated posteroventrally (0), orientated dorsoventrally (1). 0 --> 1
- Character 66 - Quadrate, shape in lateral view: curved i.e. anteriorly convex, posteriorly concave (0), straight (1). 0 --> 1
- Character 67 - Quadrate, inclination in lateral view with respect to the skull long axis: less than or equal to 10° (0), 11–30° (1), 31–45° (2), greater than 45° (3). 2 --> 0
- Character 87 - Pterygoid, anterior margin angle: posteroventral (0), dorsoventral (1), anteroventral (2). 0 --> 1
- Character 96 - Jaw, position of articulation relative to adductor fossa: posterior (0), posteromedial (1). 1 --> 0
- Character 138 - Posterior cervical vertebrae, postzygapophyses: not greatly elongated (0), greatly elongated and project posteriorly beyond the posterior centrum facet (1). 1 --> 0
- Character 140 - Cervical ribs, fused to cervical vertebrae: absent (0), present (1). 0 --> 1

- Character 158 - Dorsal ribs, shape of the proximal cross-section: triangular (0), 'L'- or 'T'-shaped (1). 1 --> 0
- Character 165 - Caudal vertebrae, attachment of haemal arches to their respective centra: articulated (0), fused (1). 0 ==> 1
- Character 182 - Posterior caudal vertebrae, shape of postzygapophyses: short with a sub-triangular end [wedge-shaped] (0), long with a rounded end [tongue-shaped] (1). 1 --> 0
- Character 184 - Posterior caudal vertebrae, shape of the haemal arches in lateral view: rounded haemal spine with no contact between haemal arches (0), inverted 'T'-shaped haemal spine with contact between the ends of adjacent spines (1). 0 ==> 1
- Character 193 - Scapula, form of the acromial process: not developed or ridge-like along the dorsal border of the scapula (0), flange-like and folded over towards the scapula glenoid (1), shelf-like and extending laterally (2), ridge terminating in a knob-like eminence (3), developed dorsally and convex upwards (4), developed dorsally and enlarged to a sharp posterodorsal corner (5). 3 ==> 2
- Character 200 - Humerus, separation of humeral head and deltopectoral crest in anterior view: continuous (0), separated by a distinct notch (1). 1 --> 0
- Character 201 - Humerus, separation of humeral head and medial tubercle in anterior view: continuous (0), separated by a distinct notch (1). 1 ==> 0
- Character 209 - Ulna, ratio of length to humerus length, less than 0.8 (0), greater than or equal to 0.8 (1). 1 --> 0
- Character 216 - Metacarpal II to humerus length ratio, less than or equal to 0.2 (0), greater than 0.2 (1). 1 --> 0
- Character 227 - Ilium, ratio of acetabular length to dorsoventral height of pubic peduncle of ilium: below 3.0 (0), 3.0 or above (1). 0 --> 1
- Character 235 - Pubis: present as separate ossification (0), fused to ilium/ischium (1). 0 --> 1
- Character 302 - Jugal/ quadratojugal 'horn', size relative to orbit size: length of base of horn equal to or less than length of orbit (0), length of base of 'horn' greater than length of orbit (1). 0 ==> 1
- Character 303 - Jugal/ quadratojugal 'horn': obscures ventral-most point of quadrate in lateral view (0), does not obscure (1). 1 --> 0
- Character 304 - Jugal/ quadratojugal 'horn', maximum length relative to squamosal 'horn' length: shorter (0), equal to or longer (1). 0 --> 1
- Character 315 - Basal surface of osteoderms: flat or gently concave (0), deeply excavated (1). 0 ==> 1
- Character 320 - Cervical half rings, distal spines: absent (0), present (1). 0 --> 1

## Vectipelta barretti measurements

Primary source: Direct measurement

Measurements = mm

	Length max	Anterior W	Anterior H	Posterior W	Posterior H	~NC H Ant	~NC H Post	Total height
--	------------	------------	------------	-------------	-------------	-----------	------------	--------------

Length Max = measured at ventral margin of centrum

### Cervical vertebrae

Axis	56							
Cervical 01		56	67	35	44			
Cervical 02	52	59	66	41	43			
Cervical 03	59	77	78	53	62	20		

### Dorsal vertebrae

Dorsal 01	64	77	78	59	60	26		
Dorsal 02		71	69	88	76			
Dorsal 03	76	71	64			23		
Dorsal 04	75	70	63			23		
Dorsal 05	76	73	66	67	70	25		
Dorsal 06	79	69	D	63				
Dorsal 07	80	74	74		72	26		
Dorsal 08	71	68	D	68	71	25		
Dorsal 09	75	38	61			25		
Dorsal 10	71			62				
Dorsal 11	83	64	67	65	68			

### Pre-sacral rod

	338			67.02	27.13		27.13	190
--	-----	--	--	-------	-------	--	-------	-----

### Sacrum - sections

Anterior	167			82	59			
Posterior	148					39.9		
Total	315							

### Caudals

	Length max	Anterior W	Anterior H	Posterior W	Posterior H	~NC H Ant	~NC H Post	Total height
--	------------	------------	------------	-------------	-------------	-----------	------------	--------------

Caudal 1	60	85	64	78	63	20	17
Caudal 2	59	83	63	72	65	19	17
Caudal 3	61	71	65	70	68	18	17
Caudal 4	57	70	69	67	68		162
Caudal 5	56	65	70	68	68		
Caudal 6	56	63	70	63	69	16	14
Caudal 7	59	60	64	58	64		
Caudal 8	60	57	62	58	65	13	13
Caudal 9	58	57	59	58	62	8	
Caudal 10	58	56	60	59	62		
Caudal 11	57	57	56	56	59		
Caudal 12	55	54	53	62	56		
Partial distal caudal							
Distal caudal	60	43		46		13	
Partial distal caudal		41	35			6	
Partial distal caudal		35	27			8	

	Length	Width	Height
--	--------	-------	--------

#### Scapula

Anterior			157	78	203
Proximal			161	18	143

#### Left Humerus

Humerus proximal			90	180	
Distal humerus			64	180	196

#### Ulna

Olecrannon?			87	93	118
-------------	--	--	----	----	-----

#### Iliia

Left			875		
Right			767		

#### Pubes

Left -incomplete			2	7	4
Right			4	11	5

#### Ischia

Right proximal	202	69	177
Right distal	60	33	260
Left proximal	205	73	180

#### ?Fibula

---

Distal section	82	53	150
----------------	----	----	-----

#### Metatarsal 2

---

Proximal section	72	54	94
Distal section	73	49	98

#### Recurved spines

---

Large thin spike. Flat base			
Large flat based spike. Tip missing		245	120
Very large spike. Flat base. Curved	140	132	149
	135	170	253

#### Flattened, blade-like spines

---

Large flattened spine	400	105	
Large flattened spine	330	123	
Large flattened spine	300	140	
Large flattened spine	240	100	

#### Plate

---

Plate	281		
-------	-----	--	--

#### Small spines with unexpanded bases

---

Small spine, tip missing	104.47	62.62	37.9
Small spine	74	51.65	31.73

#### Small peaked scutes

---

Large peaked scute	127	96	45
Peaked scute, tip broken	104.47	62.62	37.9
Peaked scute	94	62	47
Partial flat-based keeled osteoderm	97.14	65.33	27.25
Peaked scute	78	43	30



**Additional figures of *Vectipelta barretti***

All figures: top = textured meshes, bottom = untextured meshes

**Fig. S1. Cervical centrum.** A, dorsal; B, ventral; C, left lateral; D, right lateral; E, anterior; F, posterior.

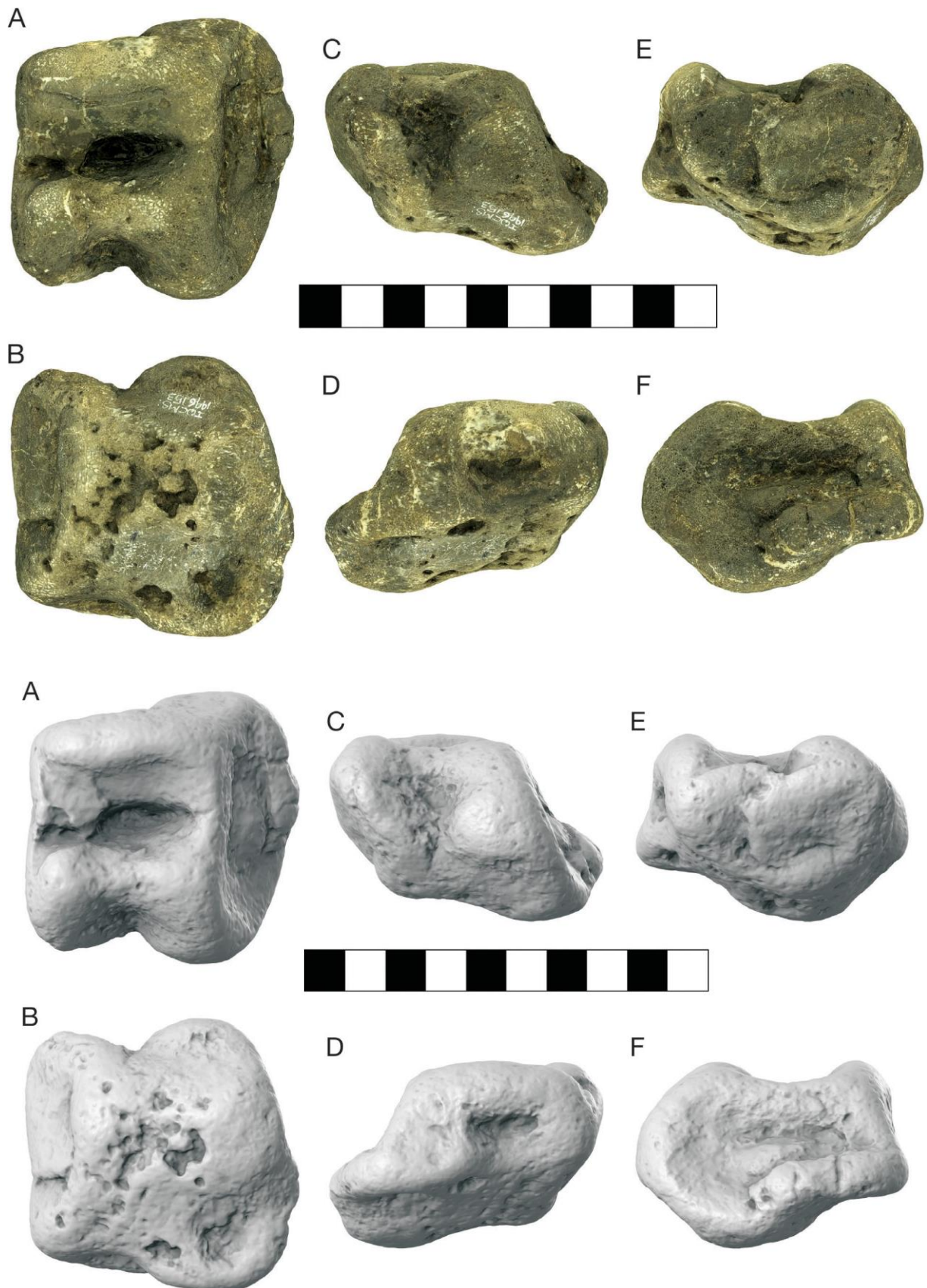


**Fig. S2. Dorsal centrum.** A, dorsal; B, ventral; C, left lateral; D, right lateral; E, anterior; F, posterior.

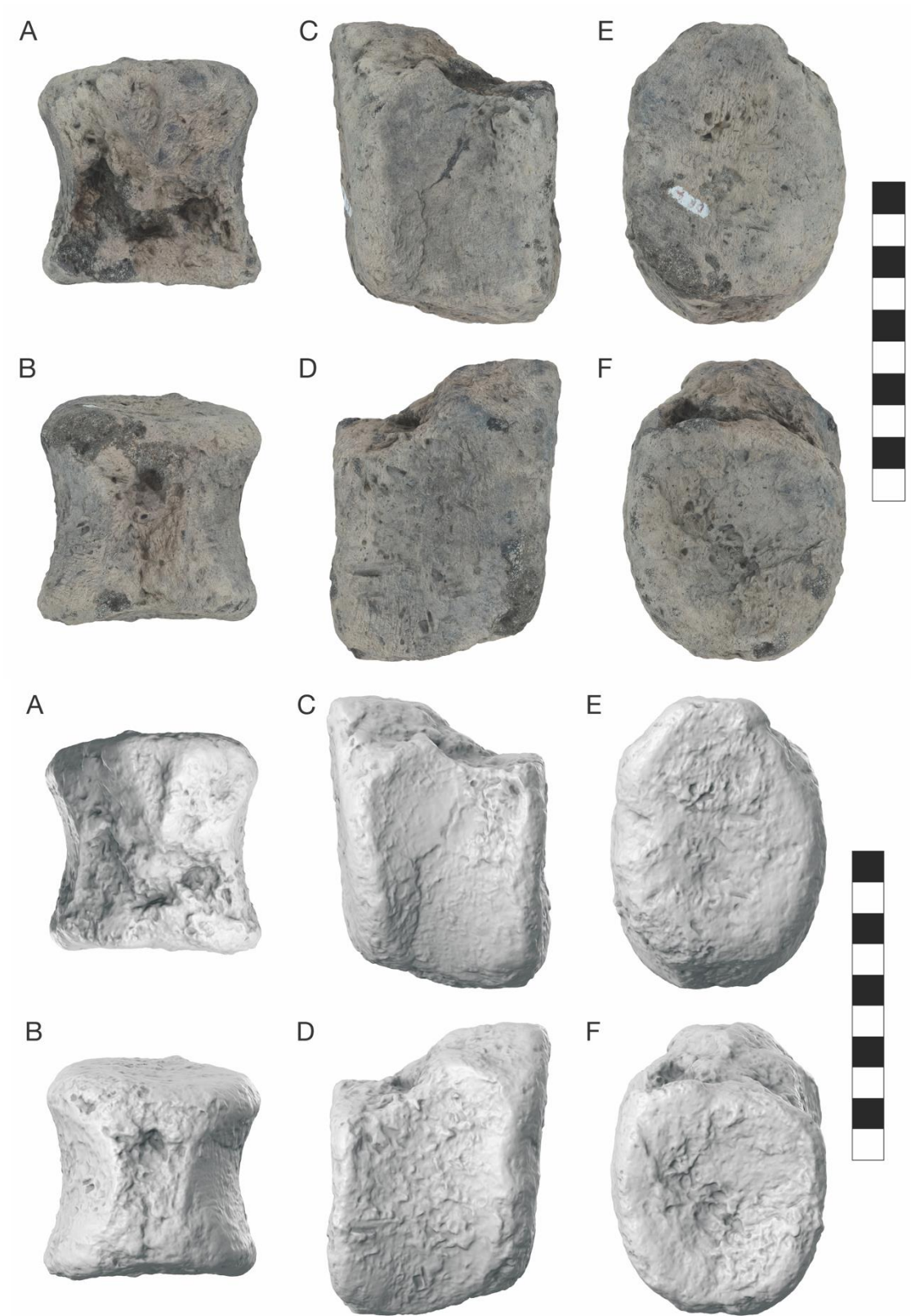


**Fig. S3. Dorsal vertebra.** A, dorsal; B, ventral; C, left lateral; D, right lateral; E, anterior; F, posterior.

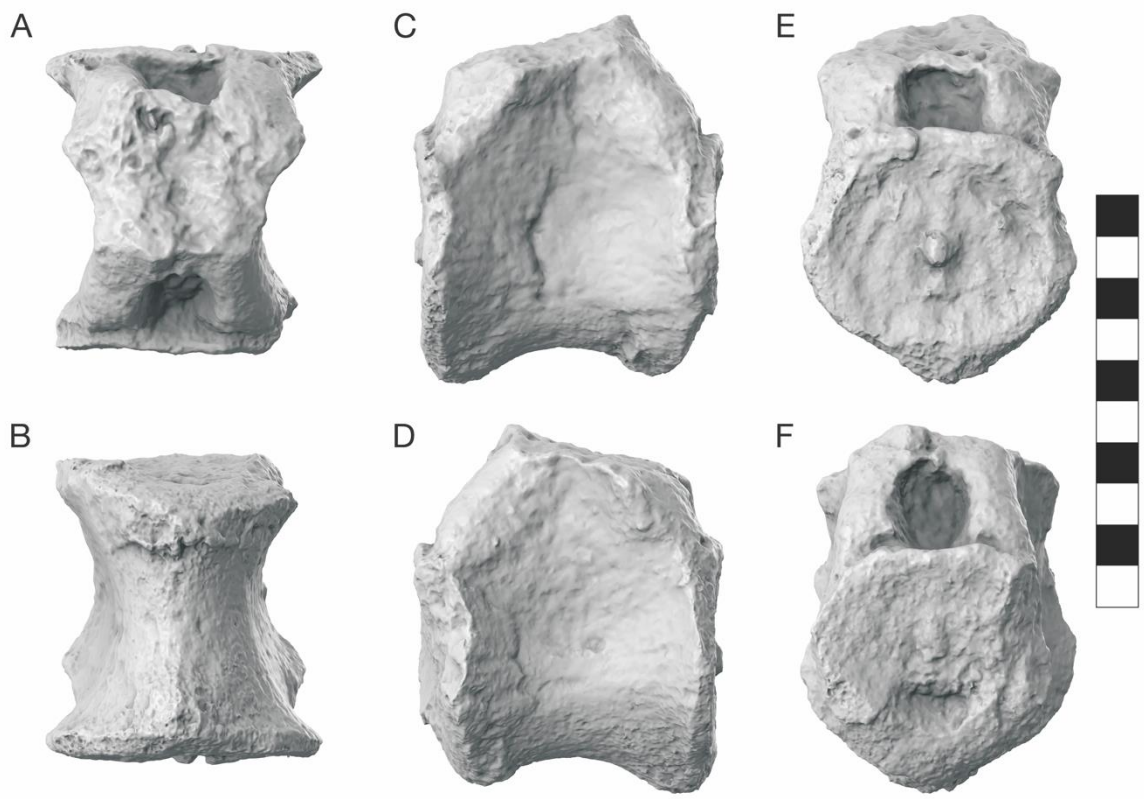
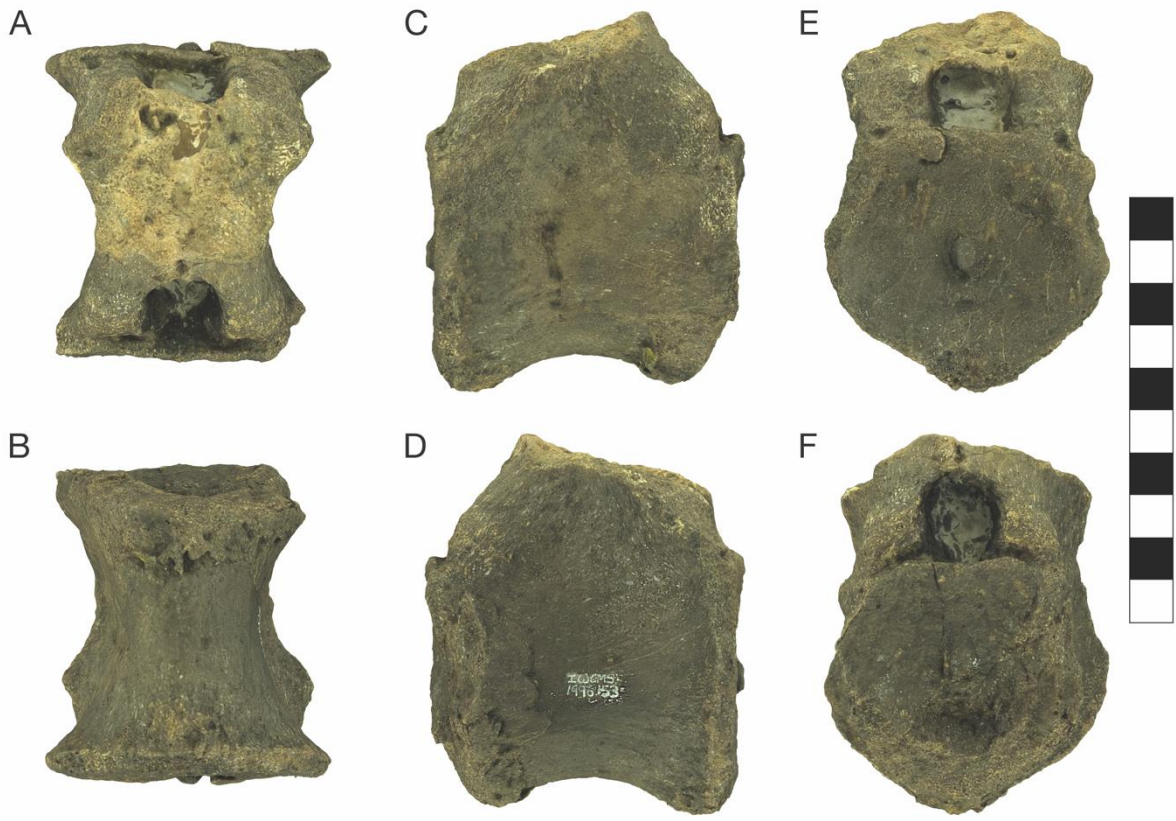


**Fig. S4. Dorsal vertebra.** A, dorsal; B, ventral; C, left lateral; D, right lateral; E, anterior; F, posterior.

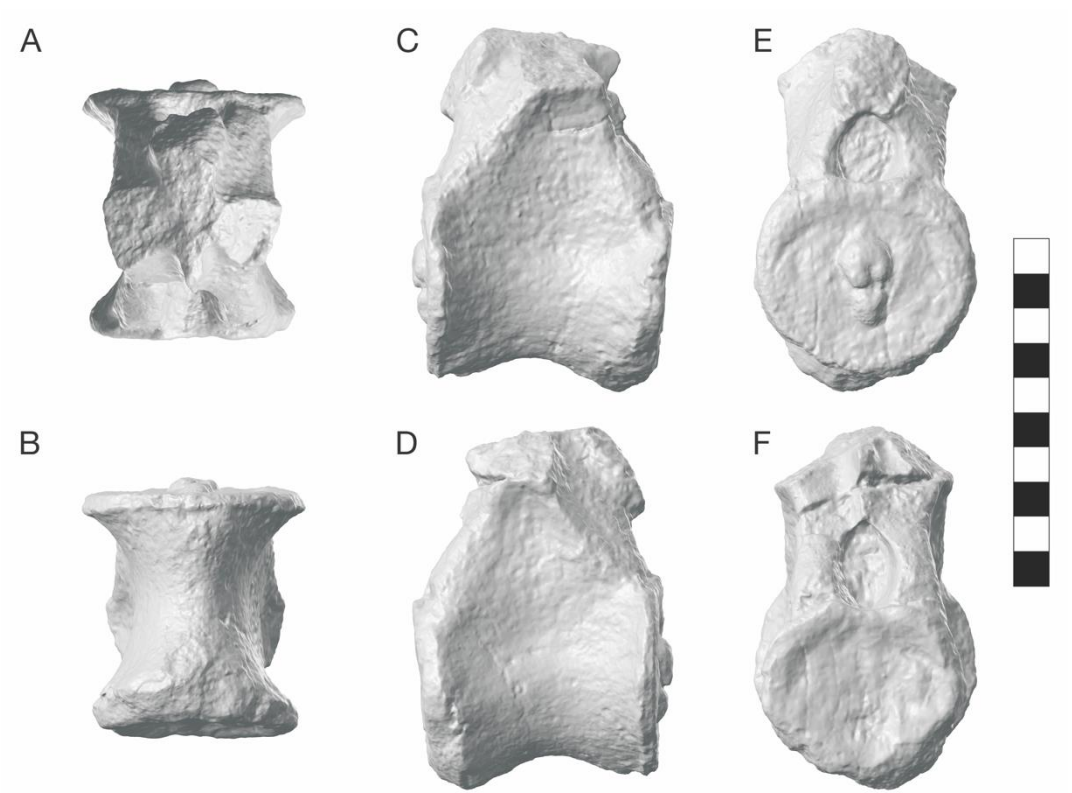
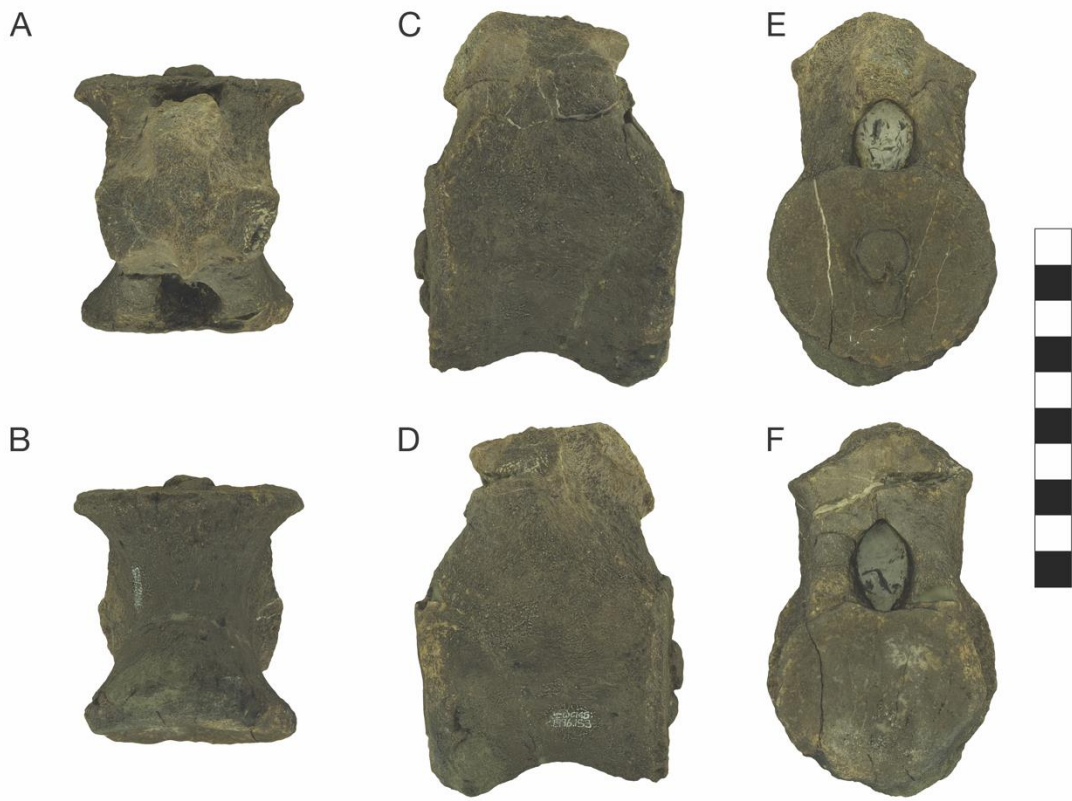


**Fig. S5. Dorsal vertebra.** A, dorsal; B, ventral; C, left lateral; D, right lateral; E, anterior; F, posterior.

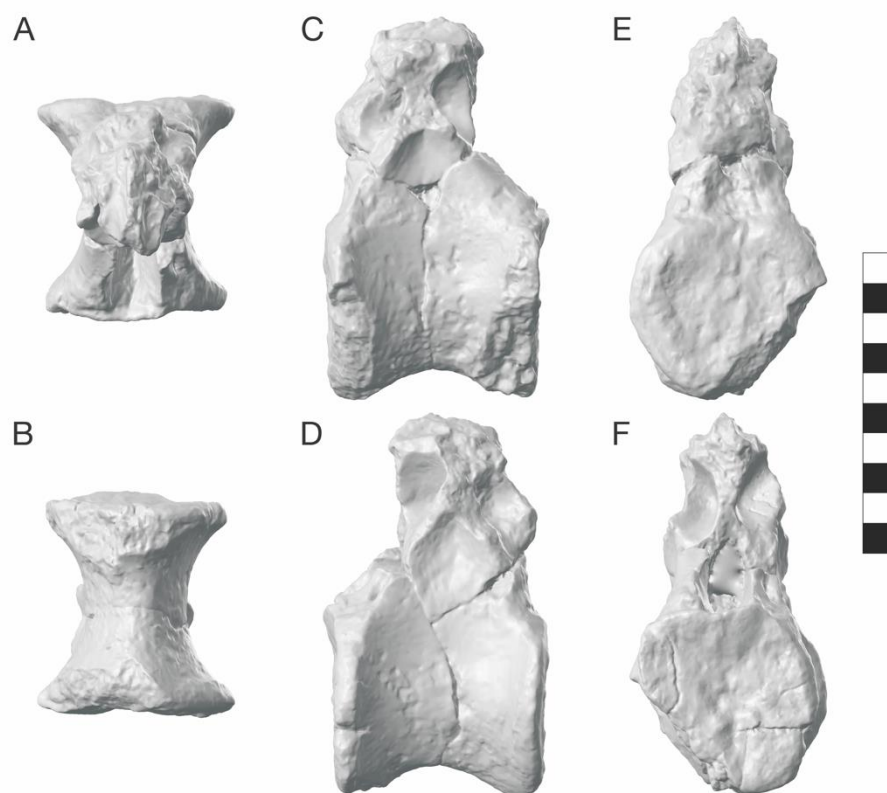
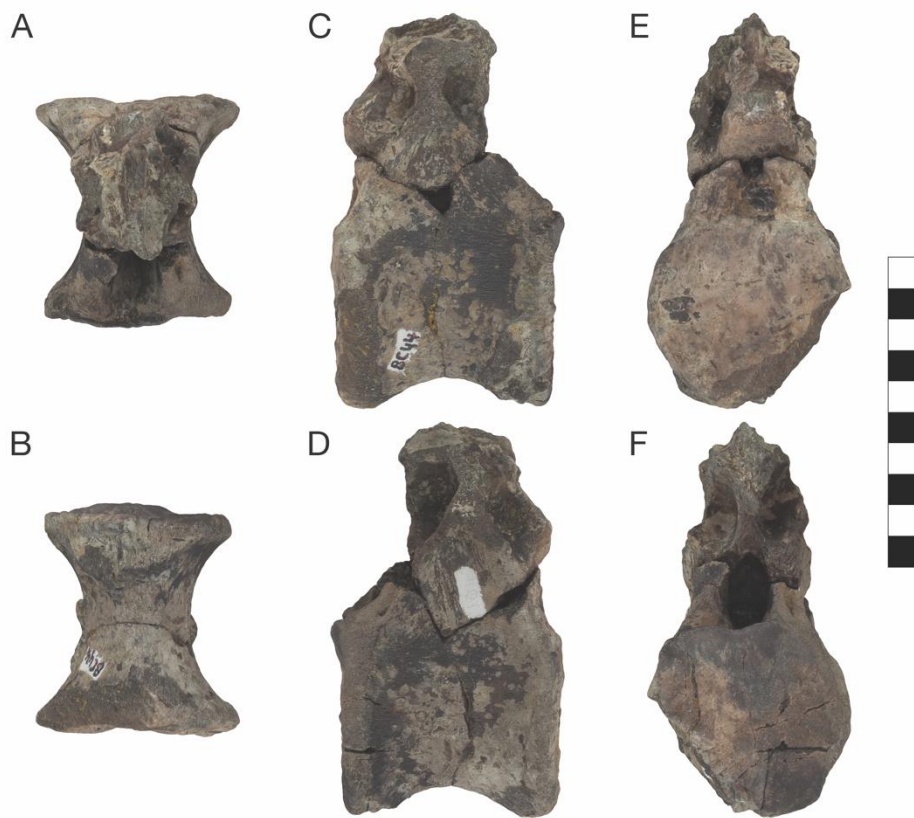


**Fig. S6. Dorsal vertebra.** A, dorsal; B, ventral; C, left lateral; D, right lateral; E, anterior; F, posterior.



**Fig. S7. Dorsal vertebra.** A, dorsal; B, ventral; C, left lateral; D, right lateral; E, anterior; F, posterior.

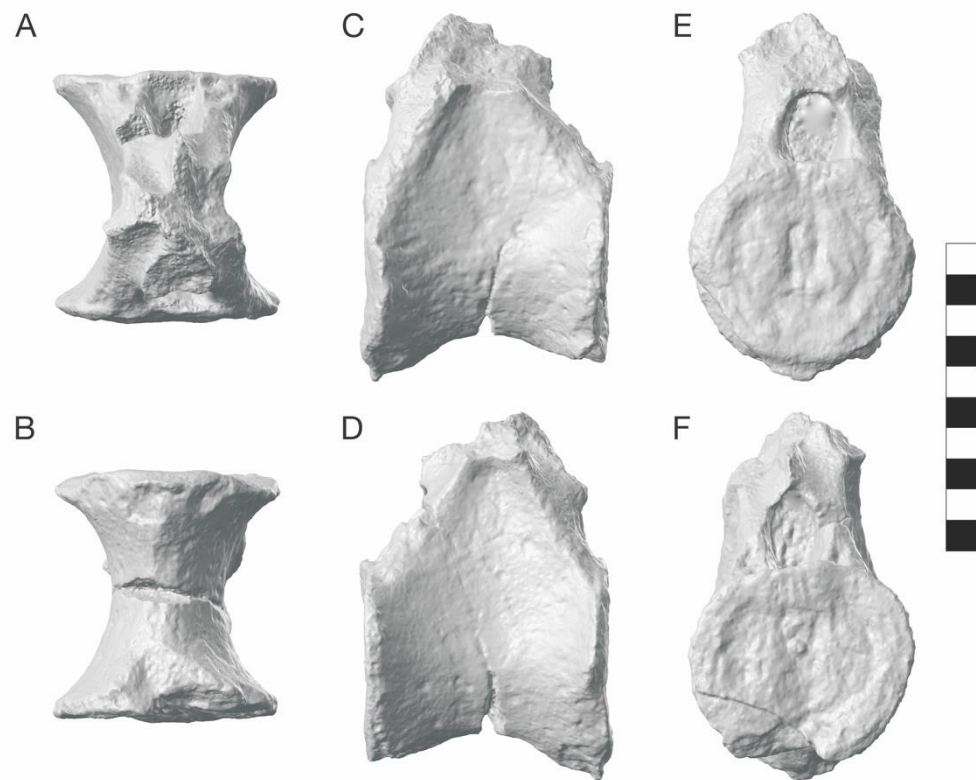
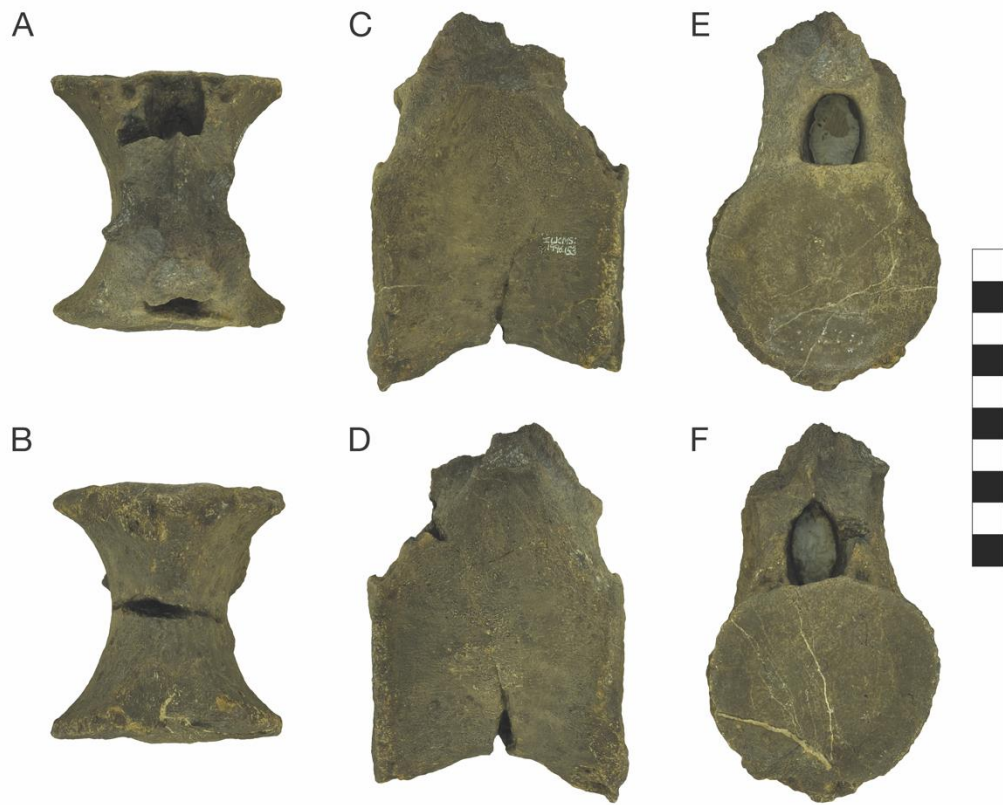


**Fig. S8. Dorsal vertebra.** A, dorsal; B, ventral; C, left lateral; D, right lateral; E, anterior; F, posterior.

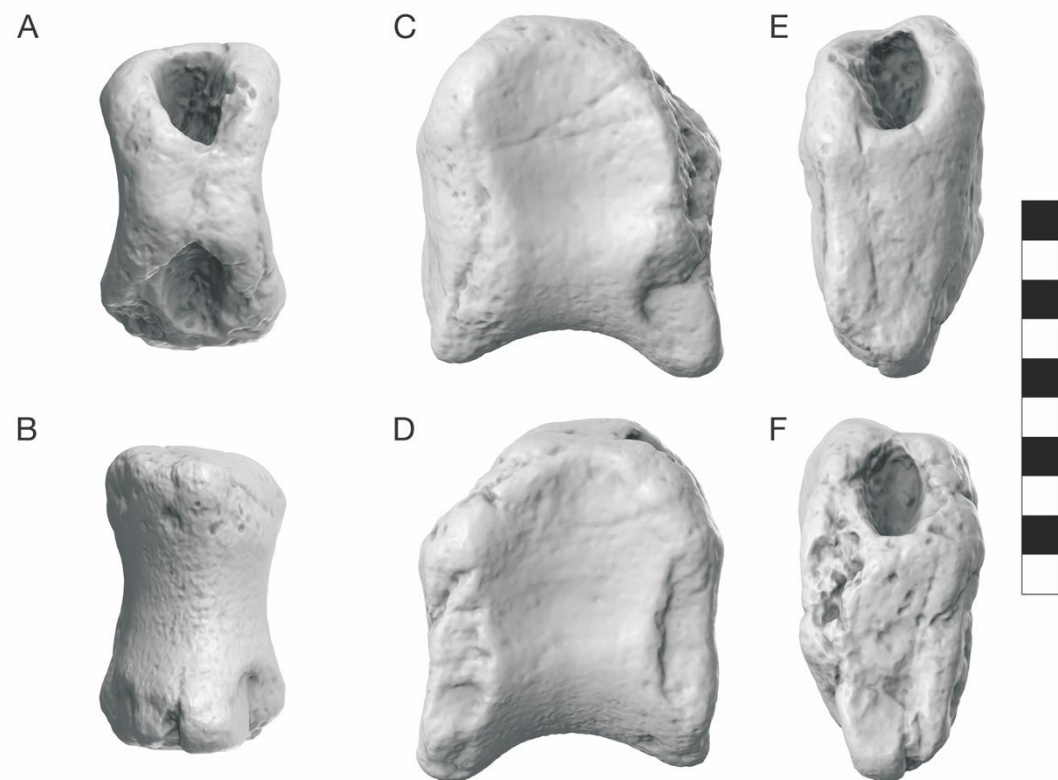
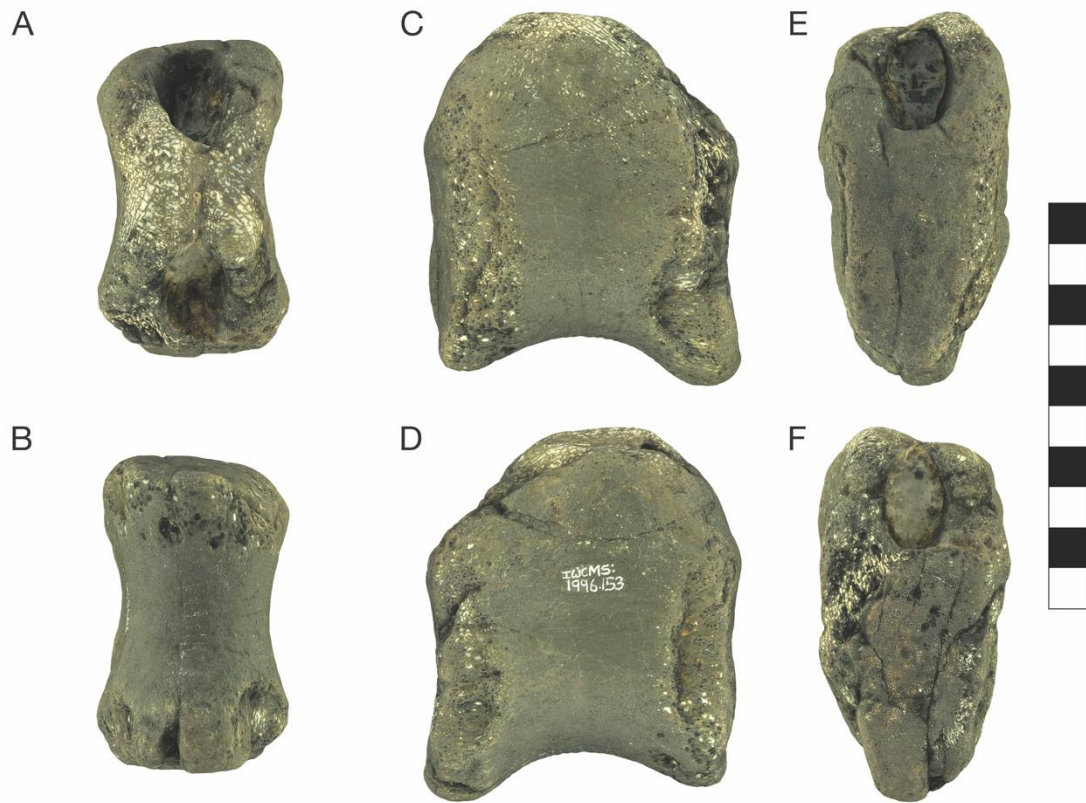


**Fig. S9. Dorsal vertebra.** A, dorsal; B, ventral; C, left lateral; D, right lateral; E, anterior; F, posterior.

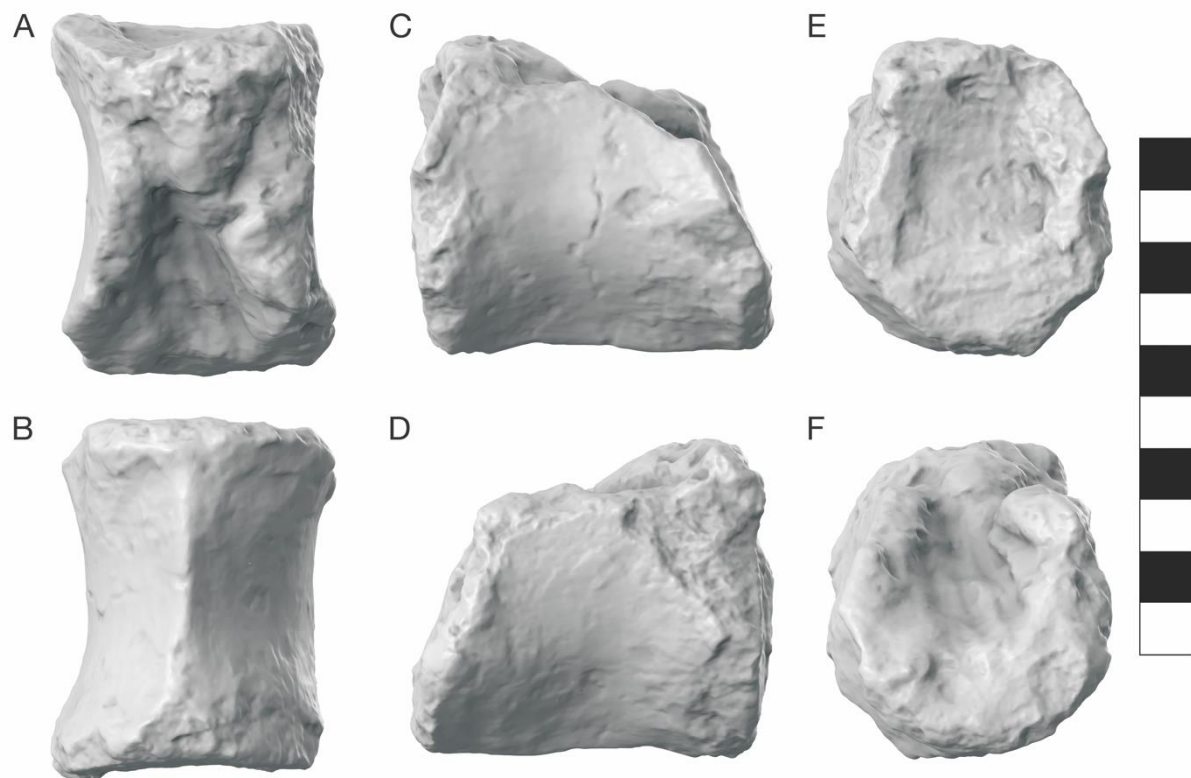
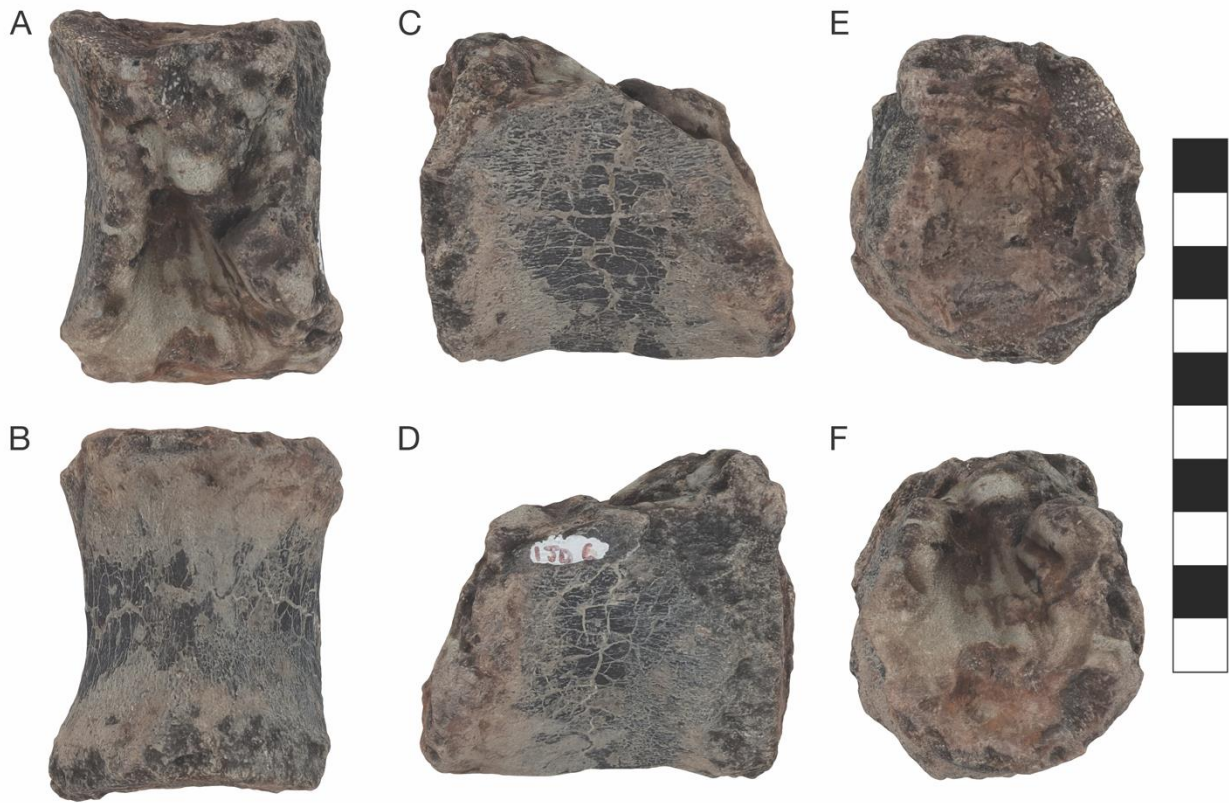


**Fig. S10. Dorsal vertebra.** A, dorsal; B, ventral; C, left lateral; D, right lateral; E, anterior; F, posterior.



**Fig. S11. Caudal vertebra.** A, dorsal; B, ventral; C, left lateral; D, right lateral; E, anterior; F, posterior.

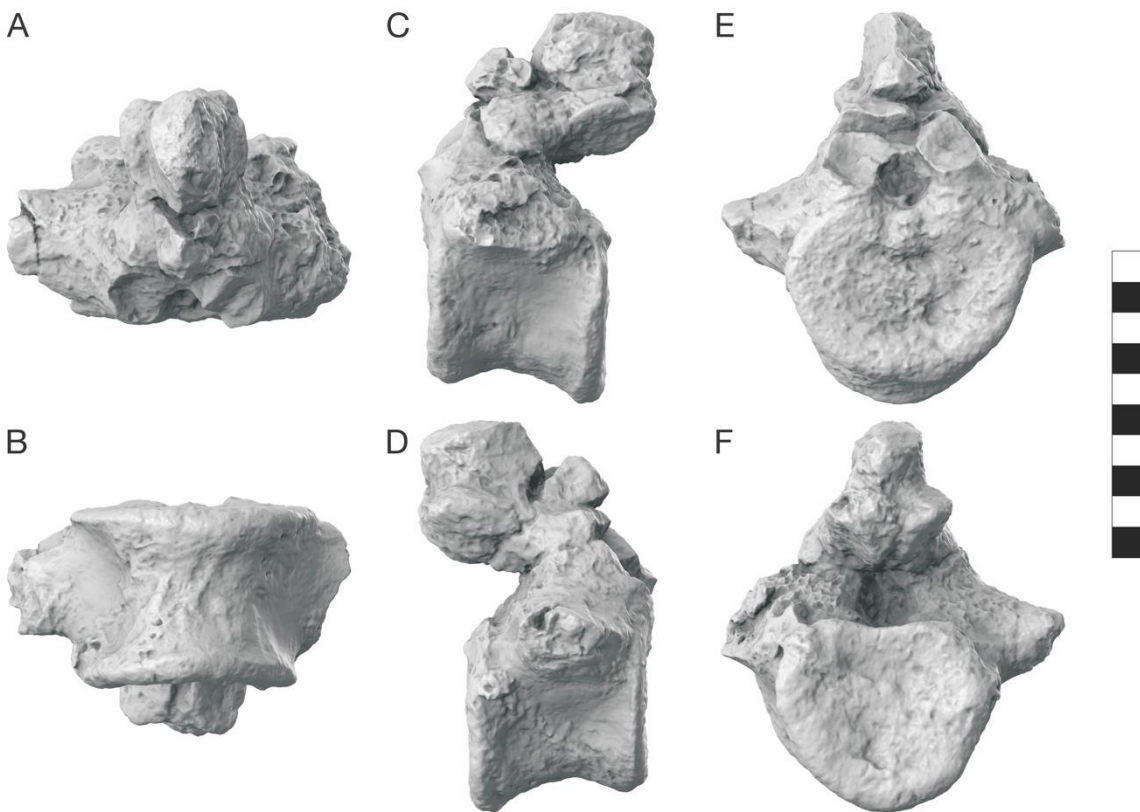
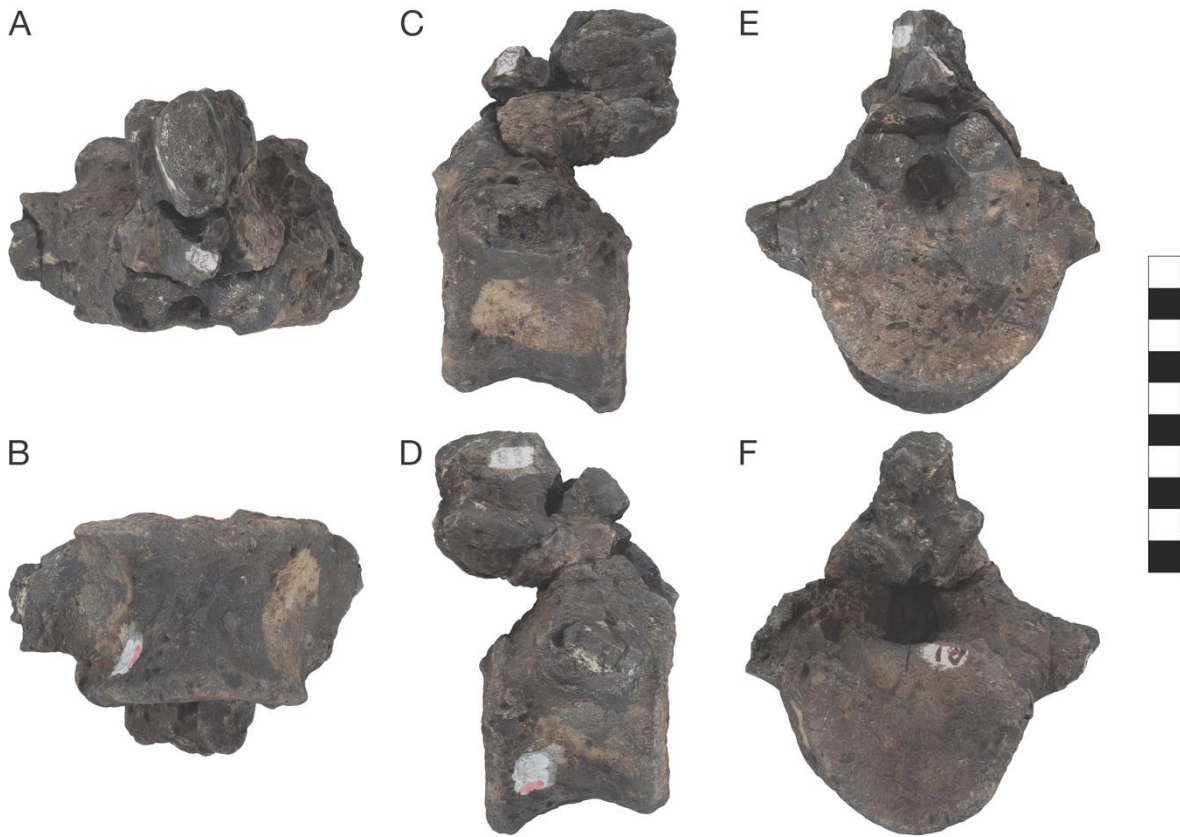


**Fig. S12. Caudal vertebra.** A, dorsal; B, ventral; C, left lateral; D, right lateral; E, anterior; F, posterior.

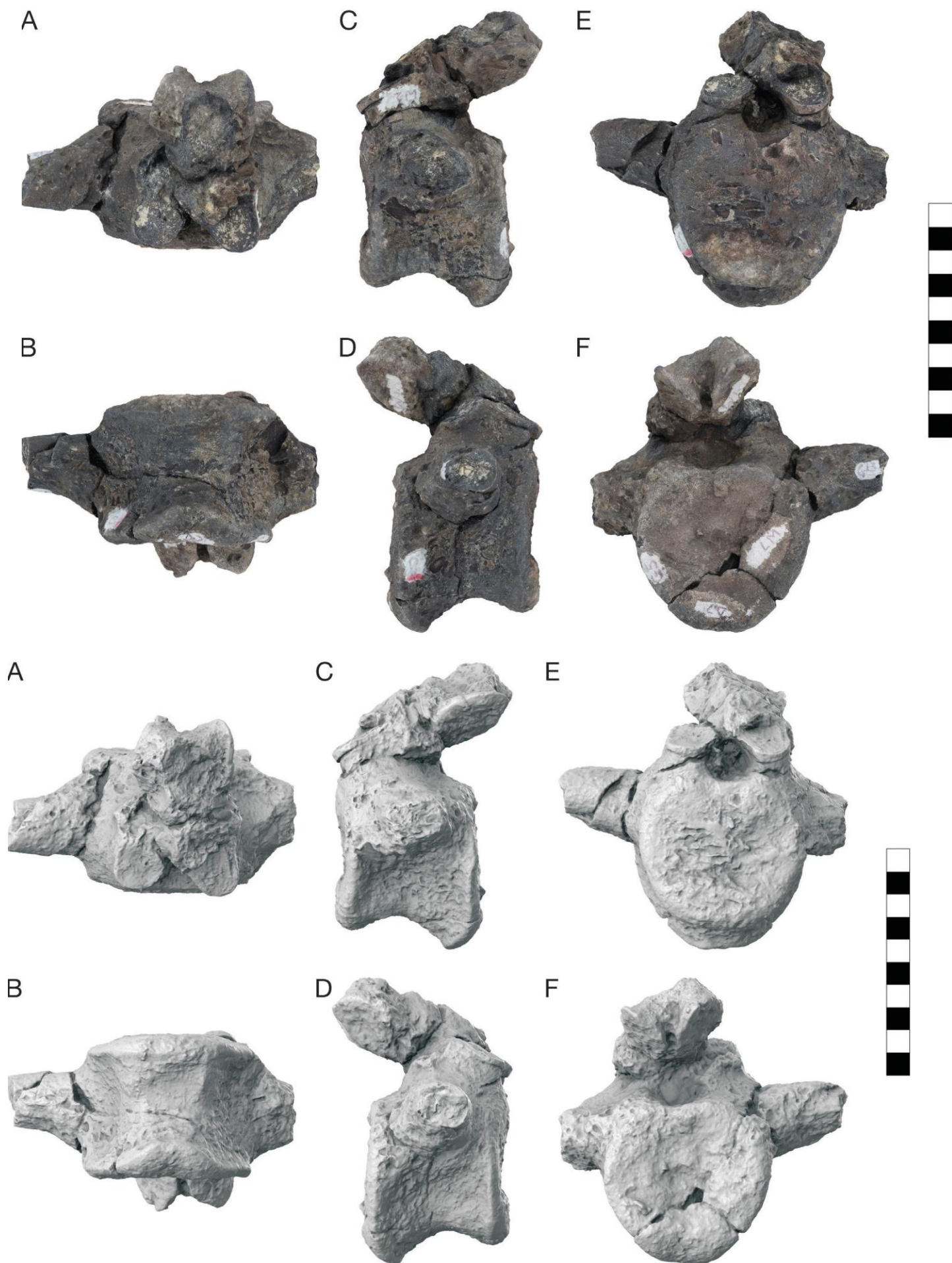


**Fig. S13. Caudal vertebra.** A, dorsal; B, ventral; C, left lateral; D, right lateral; E, anterior; F, posterior.

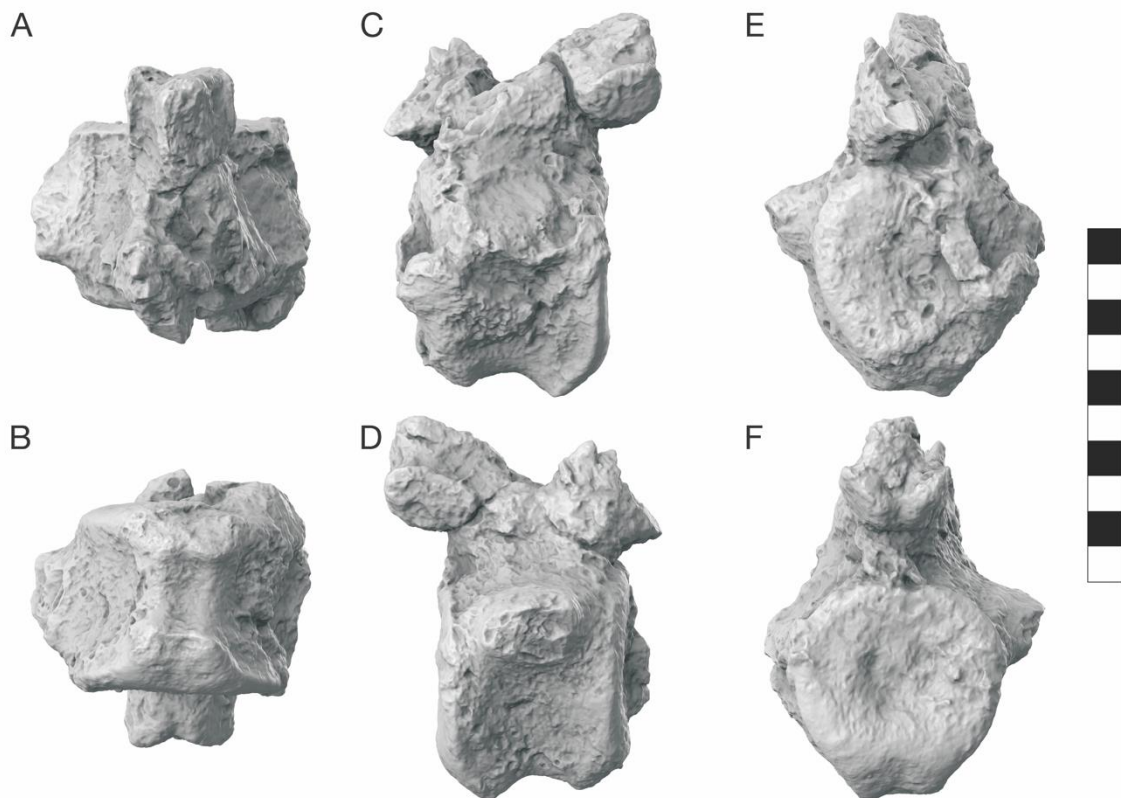
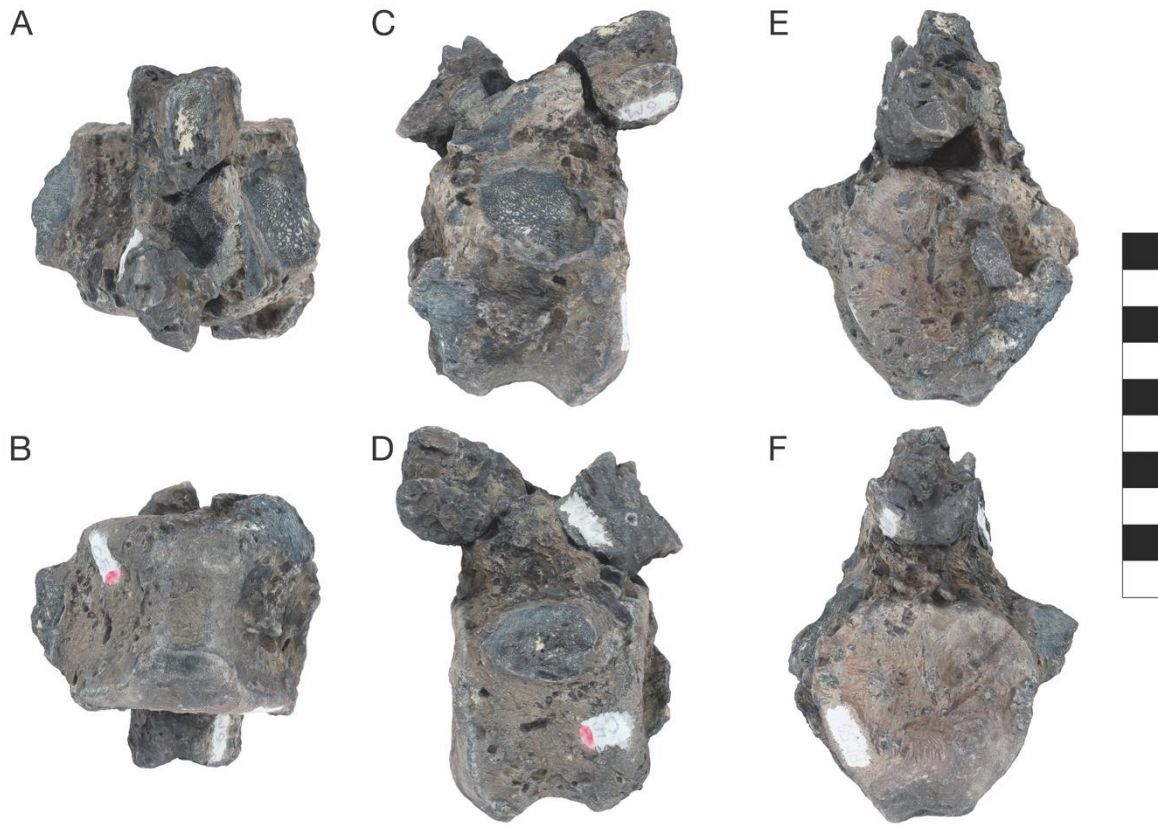


**Fig. S14. Caudal vertebra.** A, dorsal; B, ventral; C, left lateral; D, right lateral; E, anterior; F, posterior.

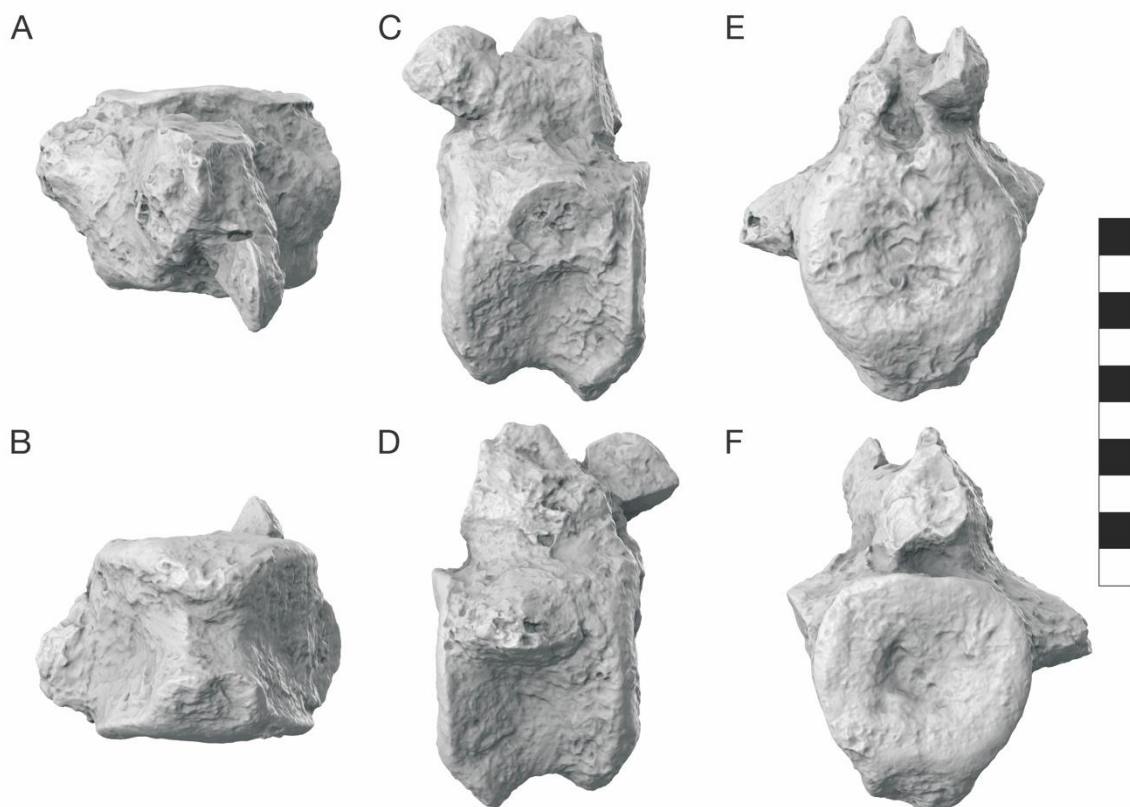
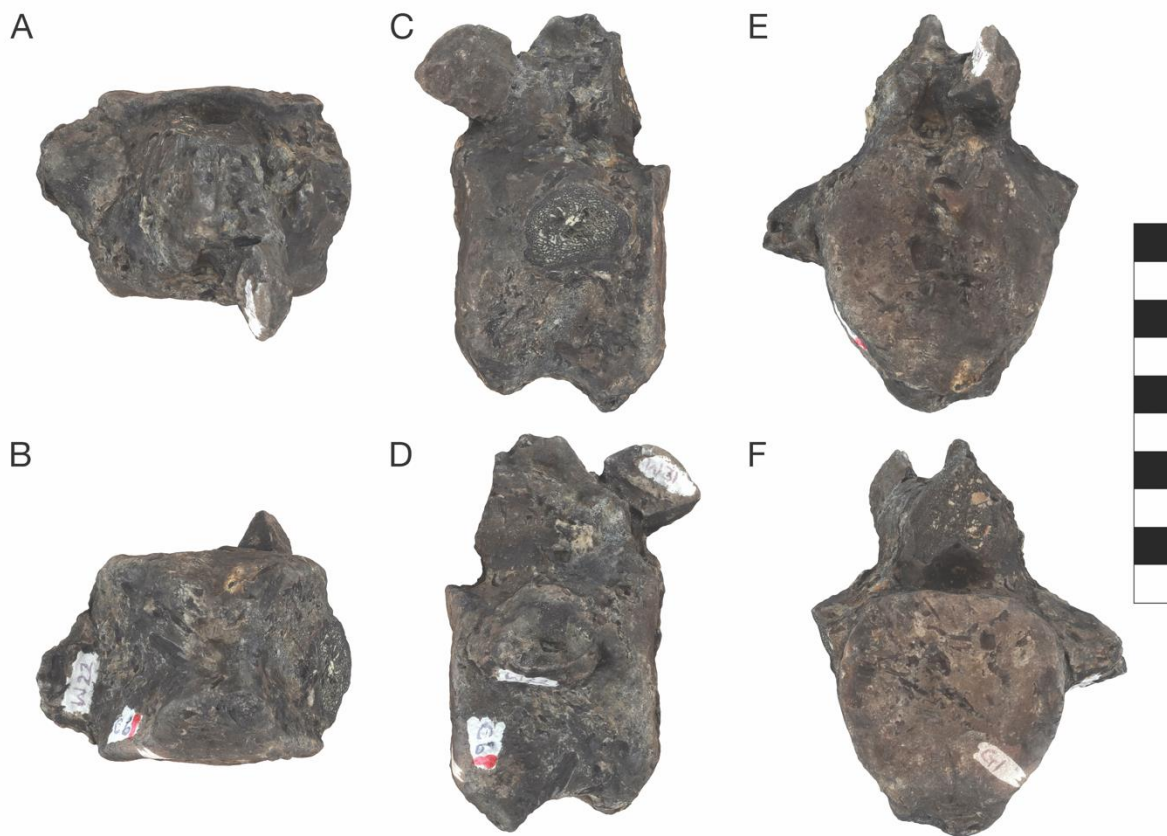


**Fig. S15. Caudal vertebra.** A, dorsal; B, ventral; C, left lateral; D, right lateral; E, anterior; F, posterior.

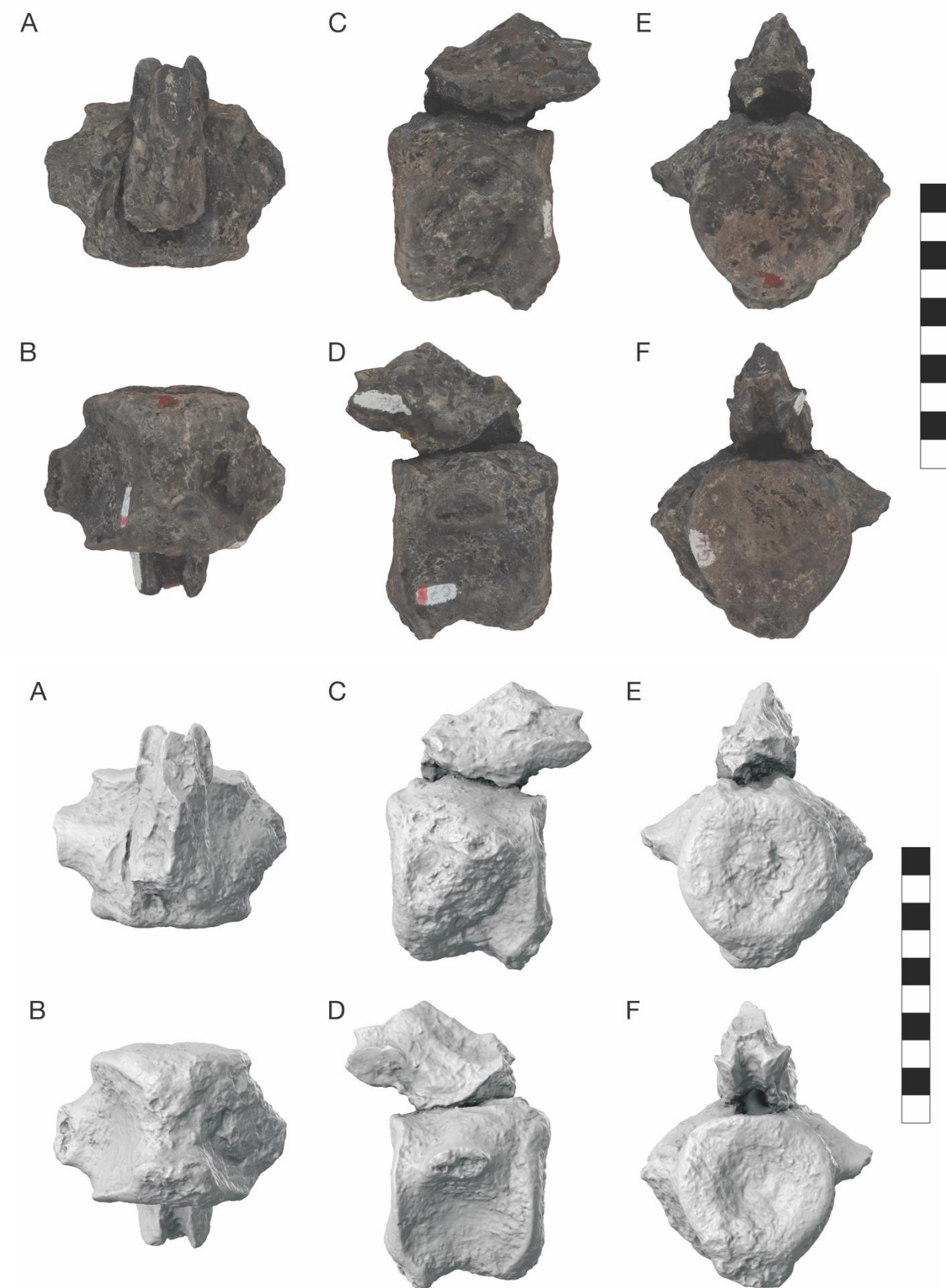


**Fig. S16. Caudal vertebra.** A, dorsal; B, ventral; C, left lateral; D, right lateral; E, anterior; F, posterior.

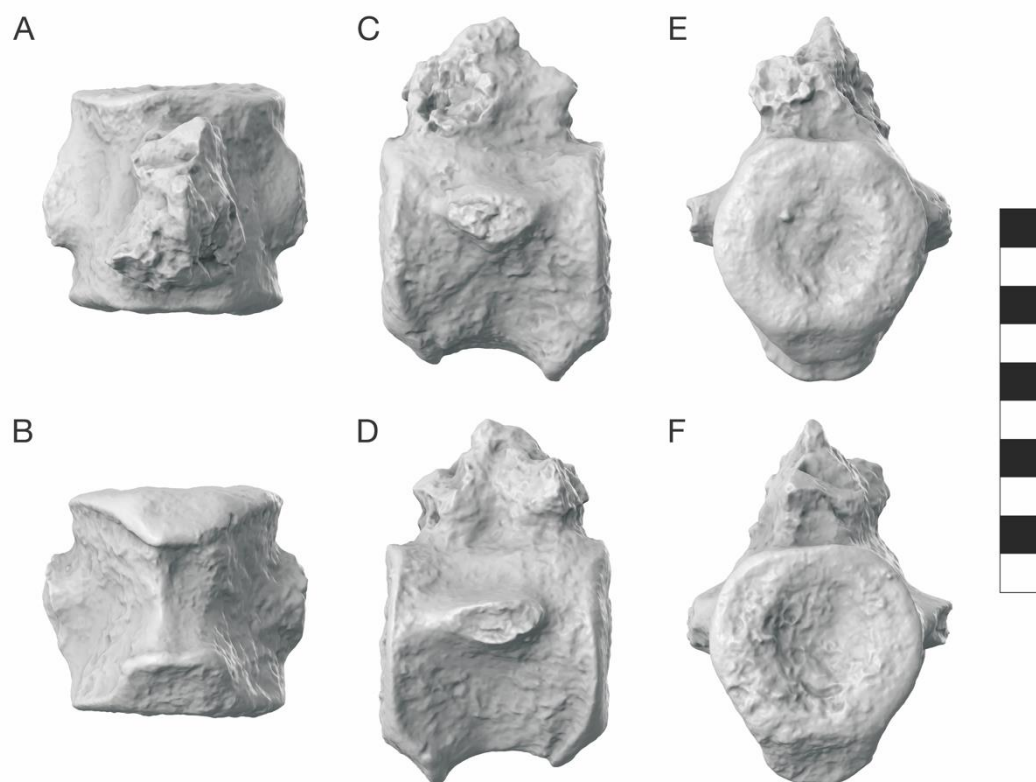
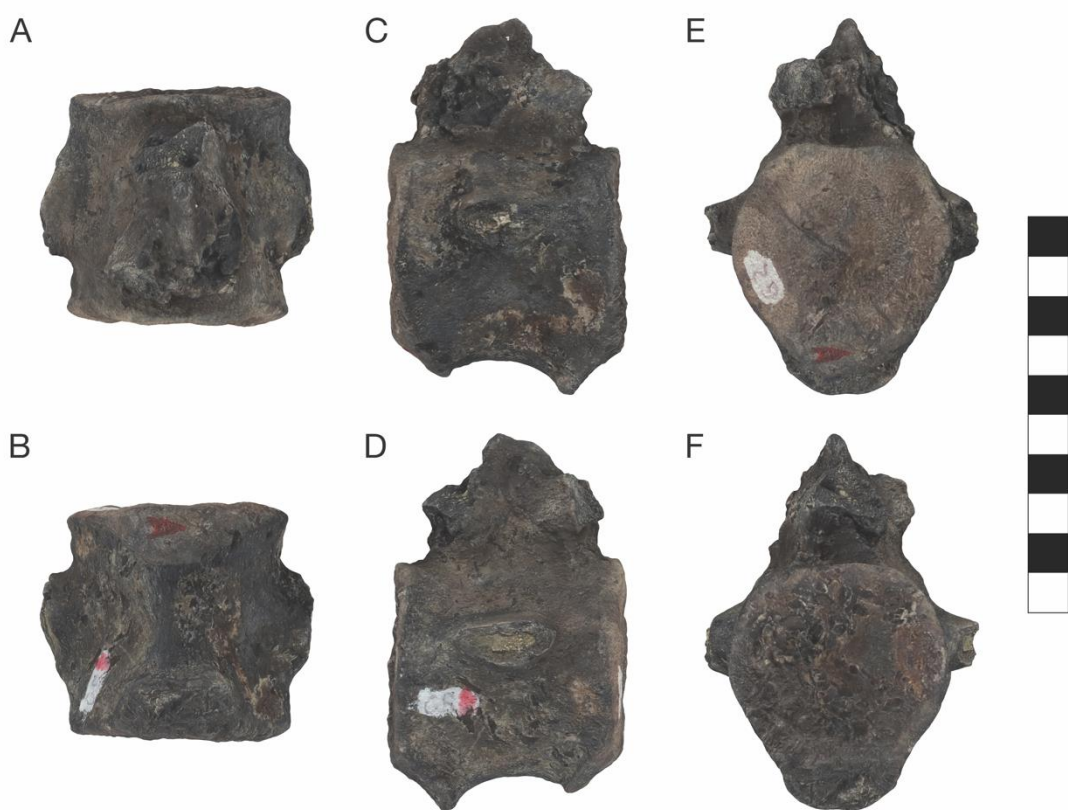


**Fig. S17. Caudal vertebra.** A, dorsal; B, ventral; C, left lateral; D, right lateral; E, anterior; F, posterior.

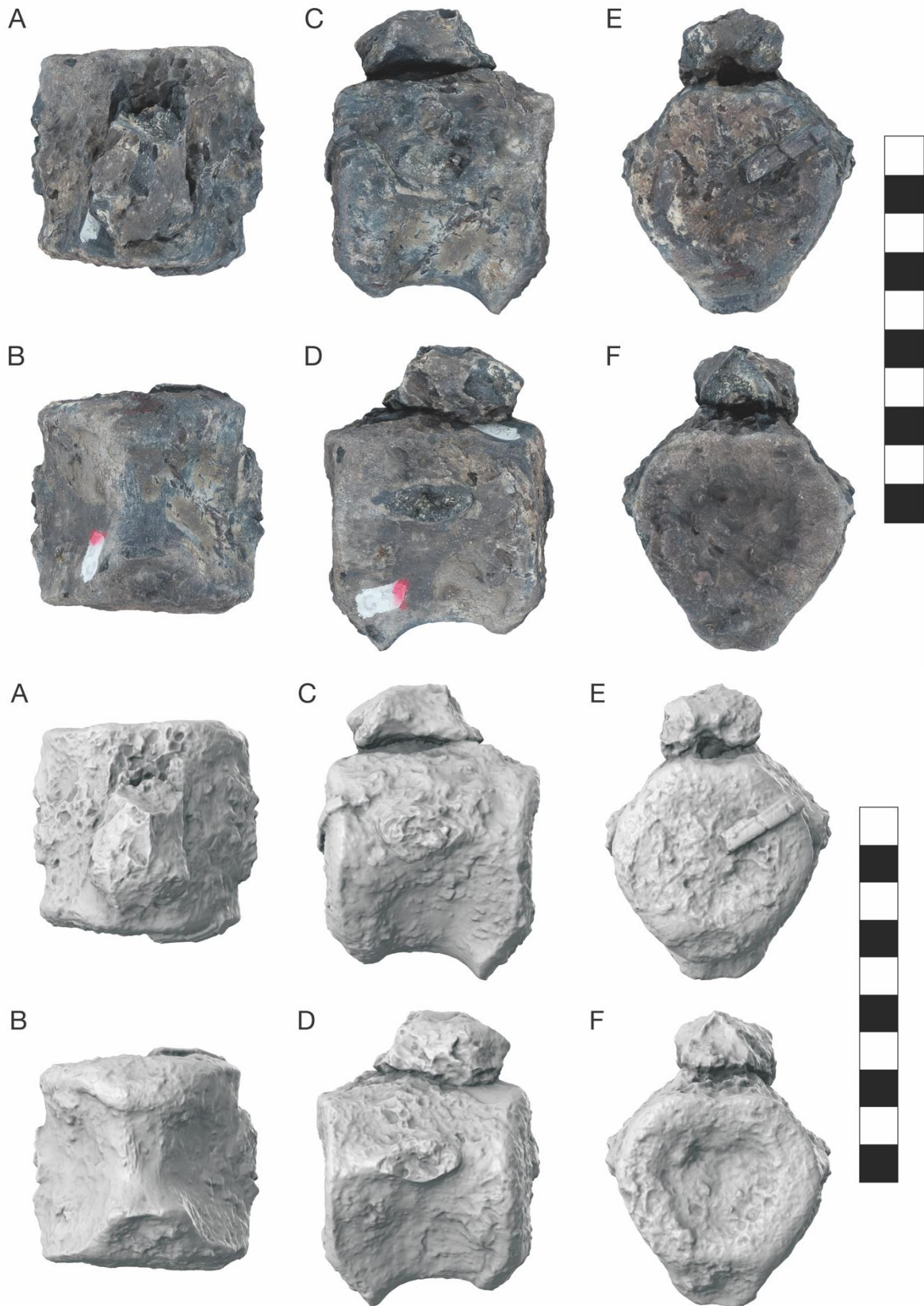


**Fig. S18. Caudal vertebra.** A, dorsal; B, ventral; C, left lateral; D, right lateral; E, anterior; F, posterior.

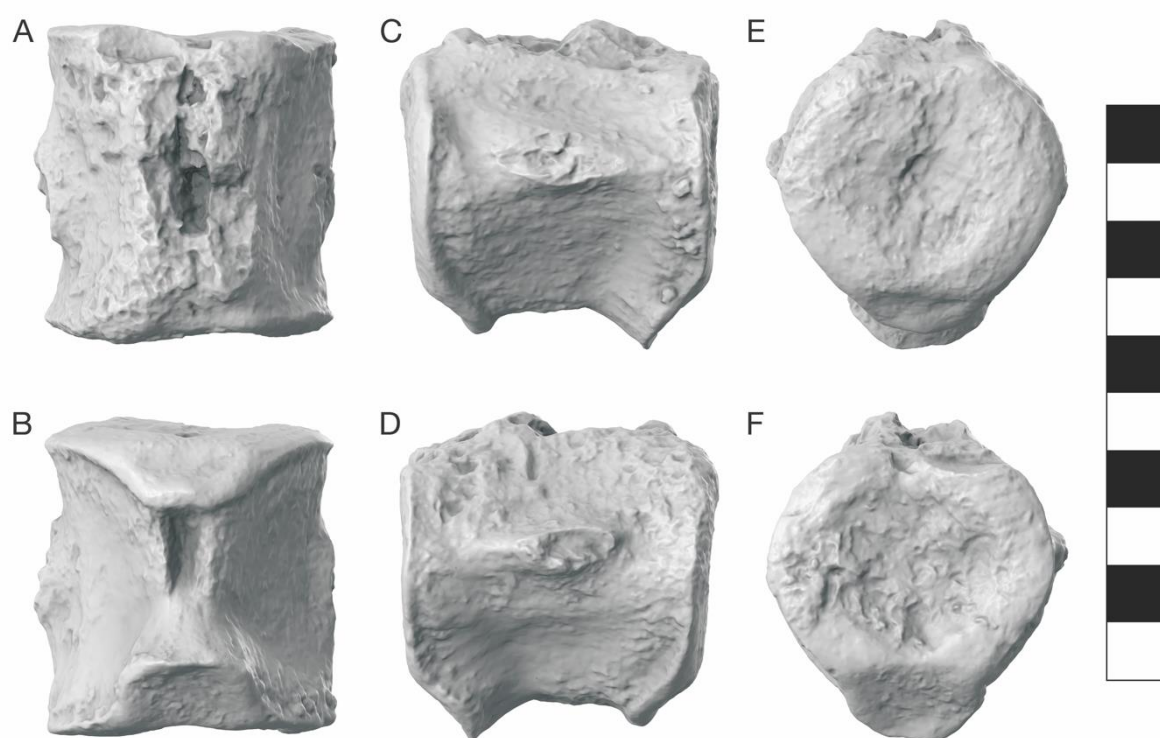
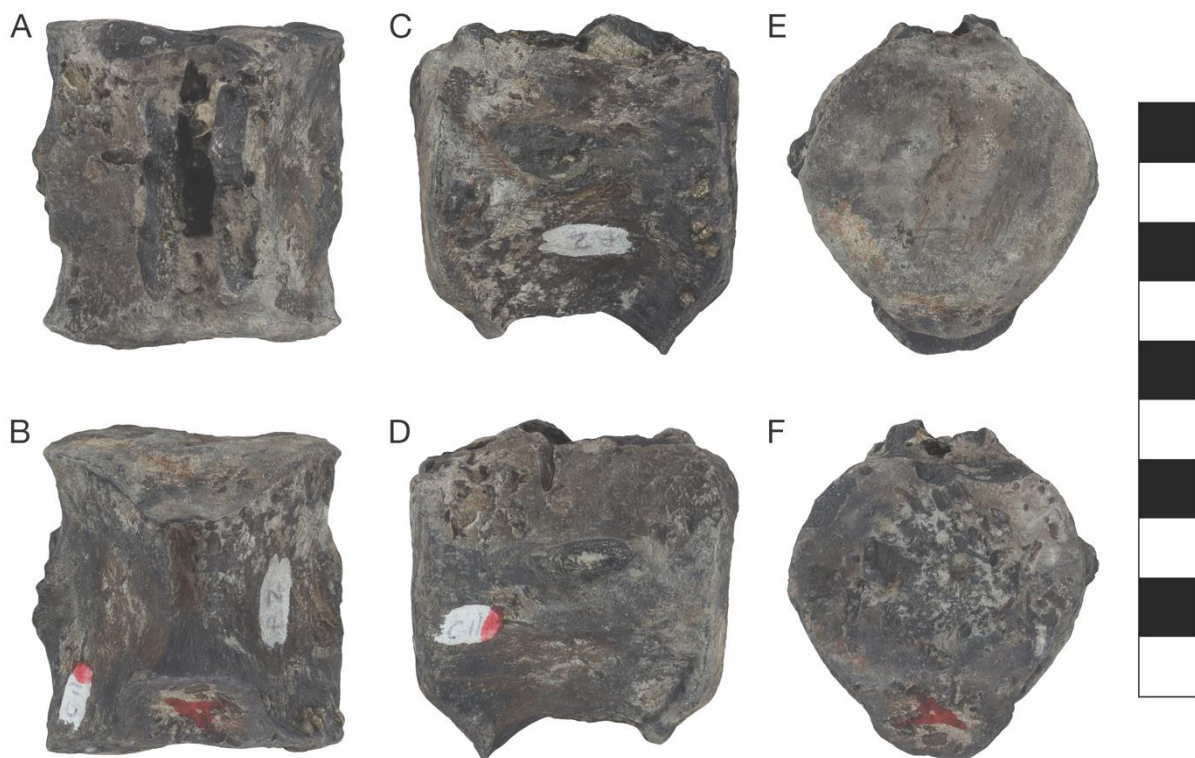


**Fig. S19. Caudal vertebra.** A, dorsal; B, ventral; C, left lateral; D, right lateral; E, anterior; F, posterior.

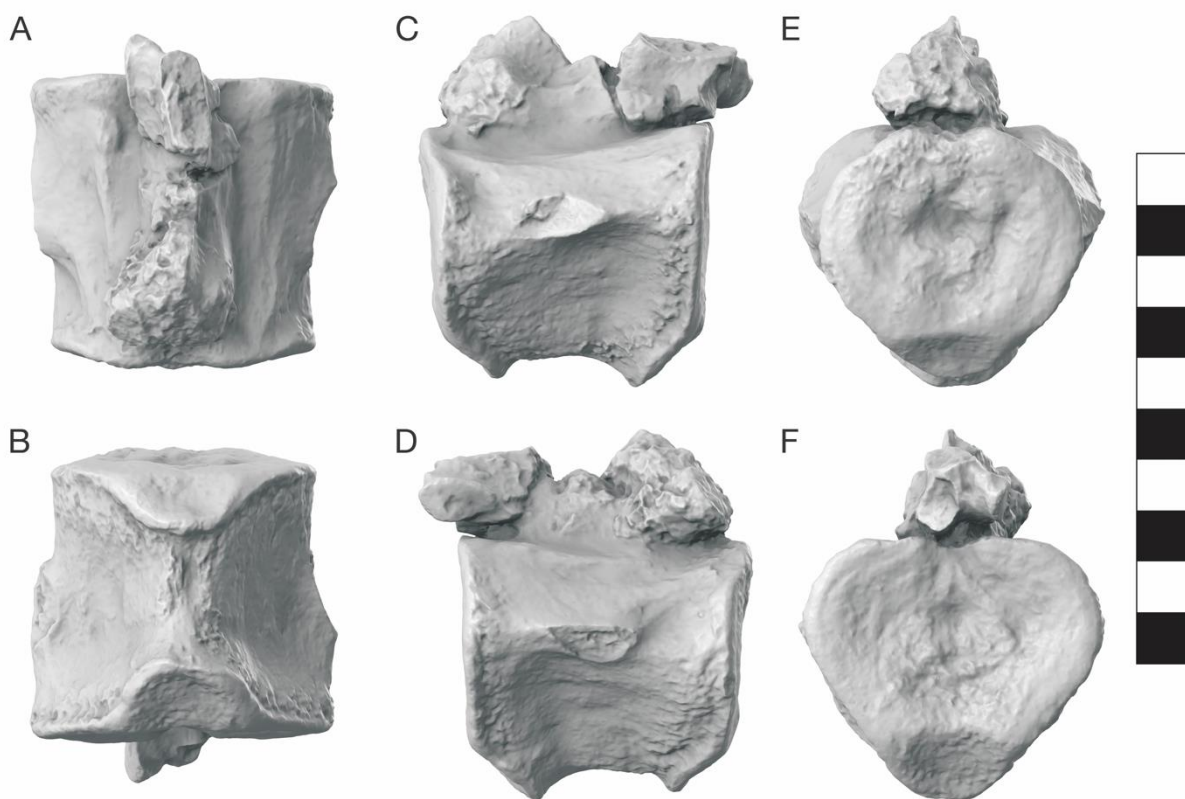
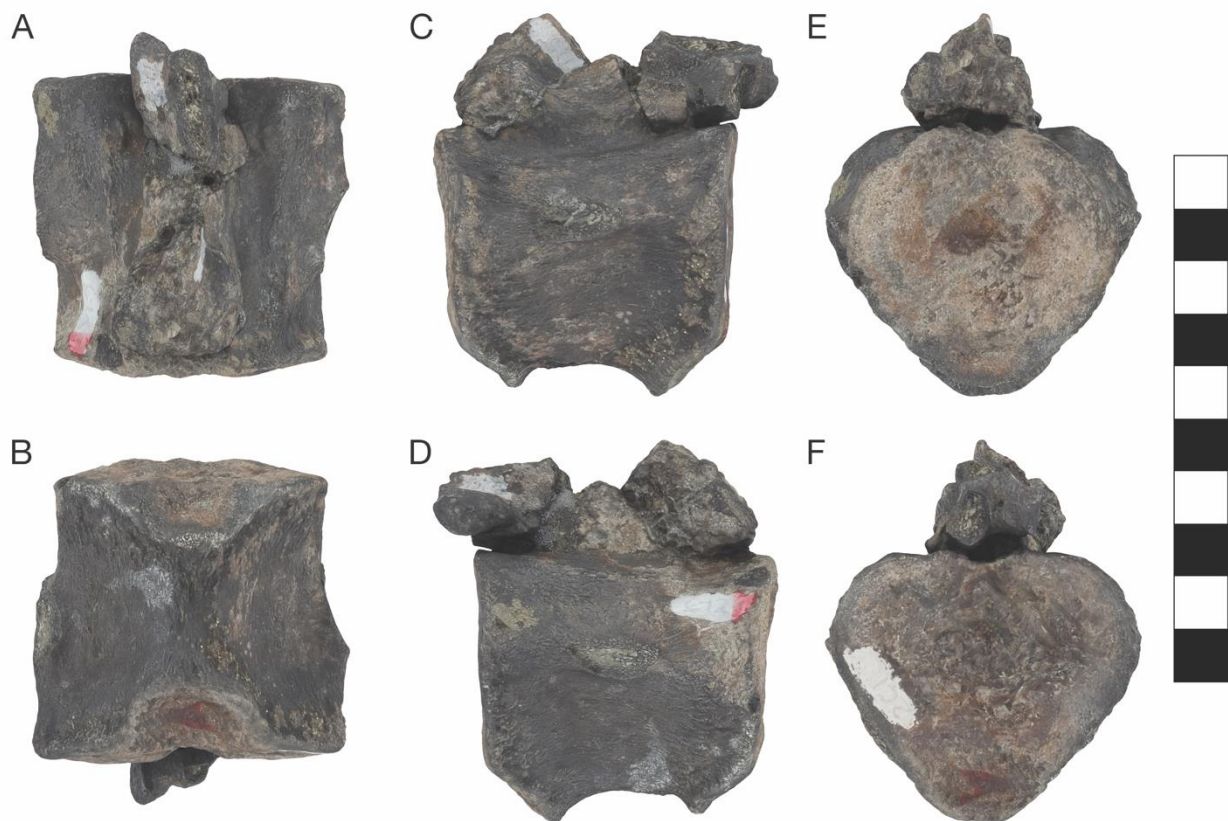


**Fig. S20. Caudal vertebra.** A, dorsal; B, ventral; C, left lateral; D, right lateral; E, anterior; F, posterior.

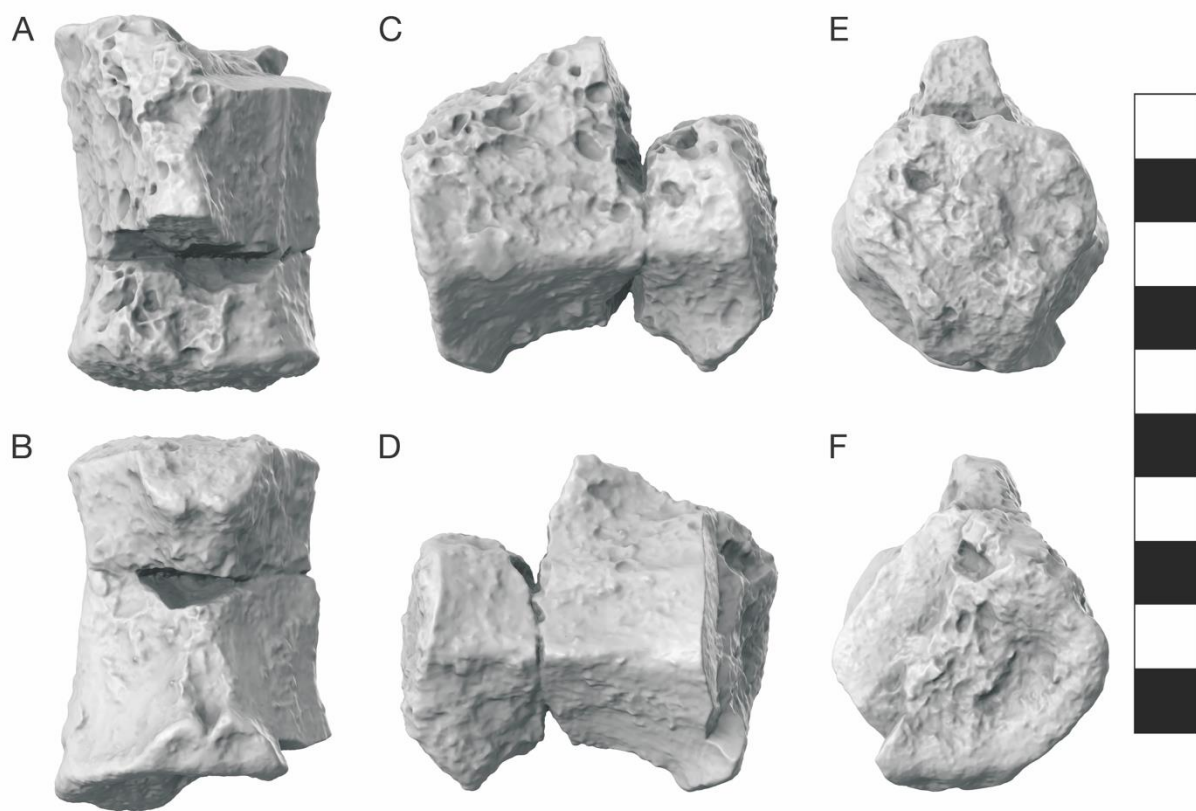
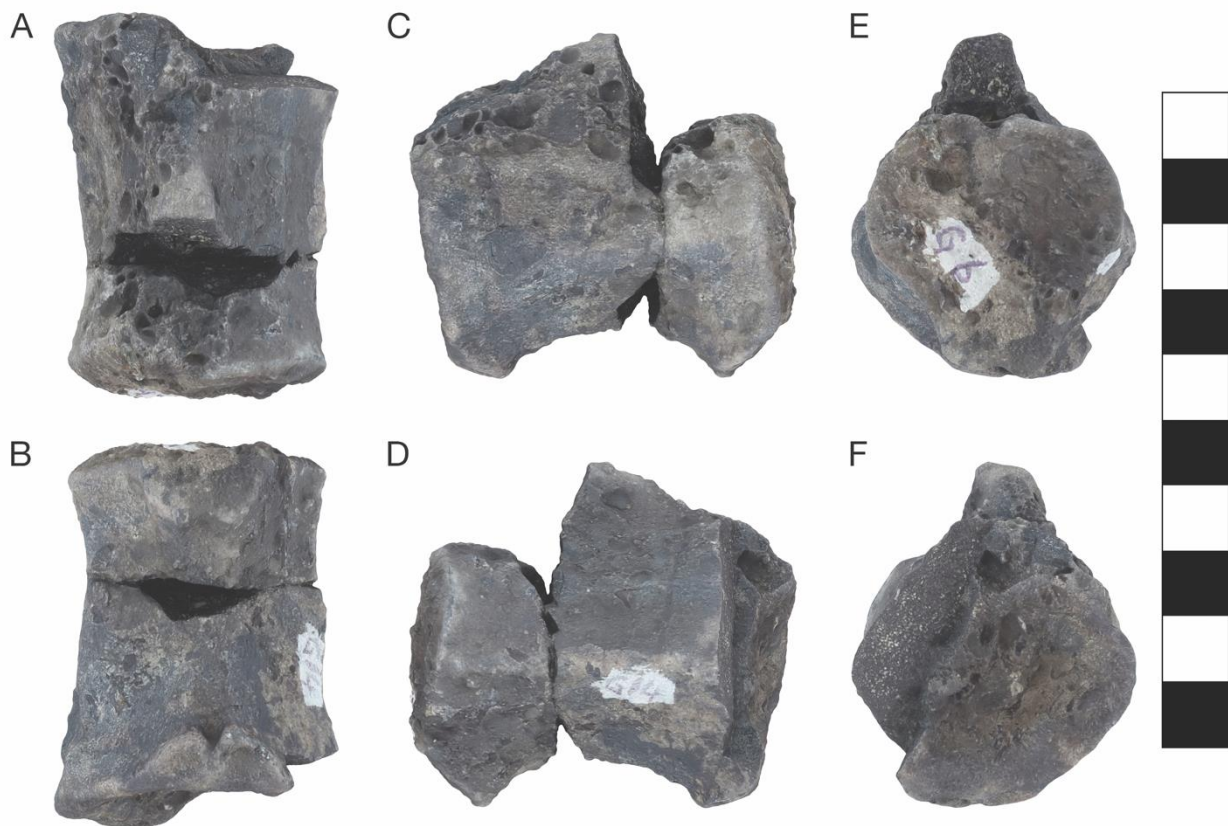


**Fig. S21. Caudal vertebra.** Orientation presumed: A, dorsal; B, ventral; C, left lateral; D, right lateral; E, anterior; F, posterior.

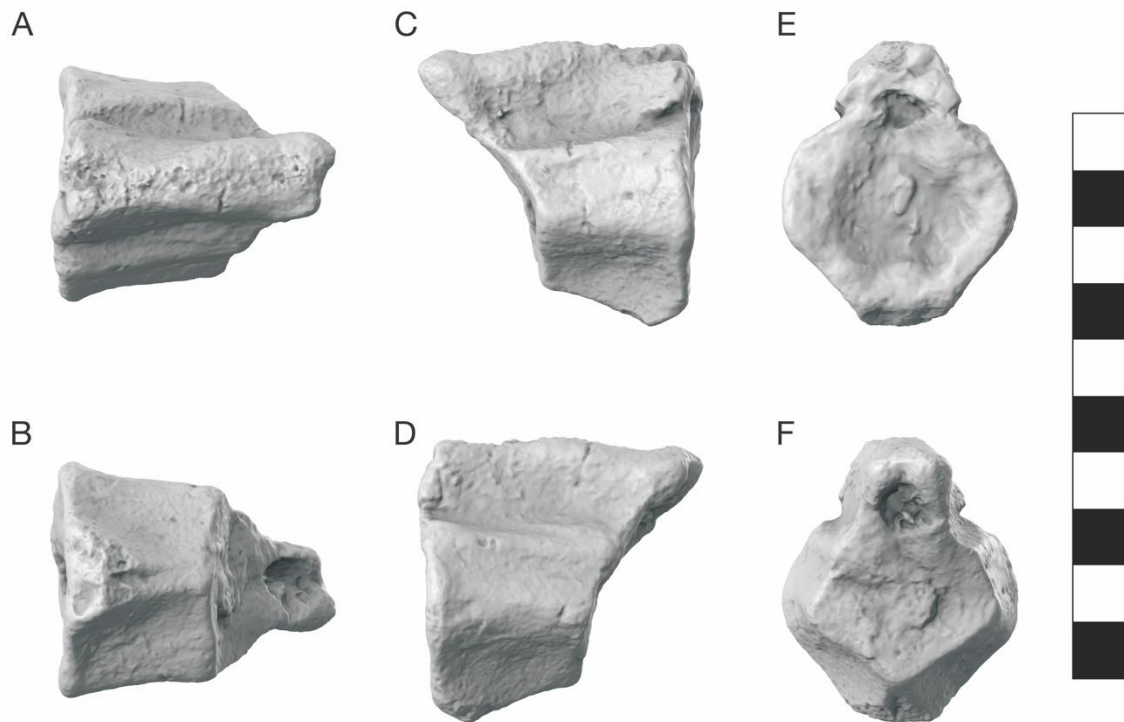
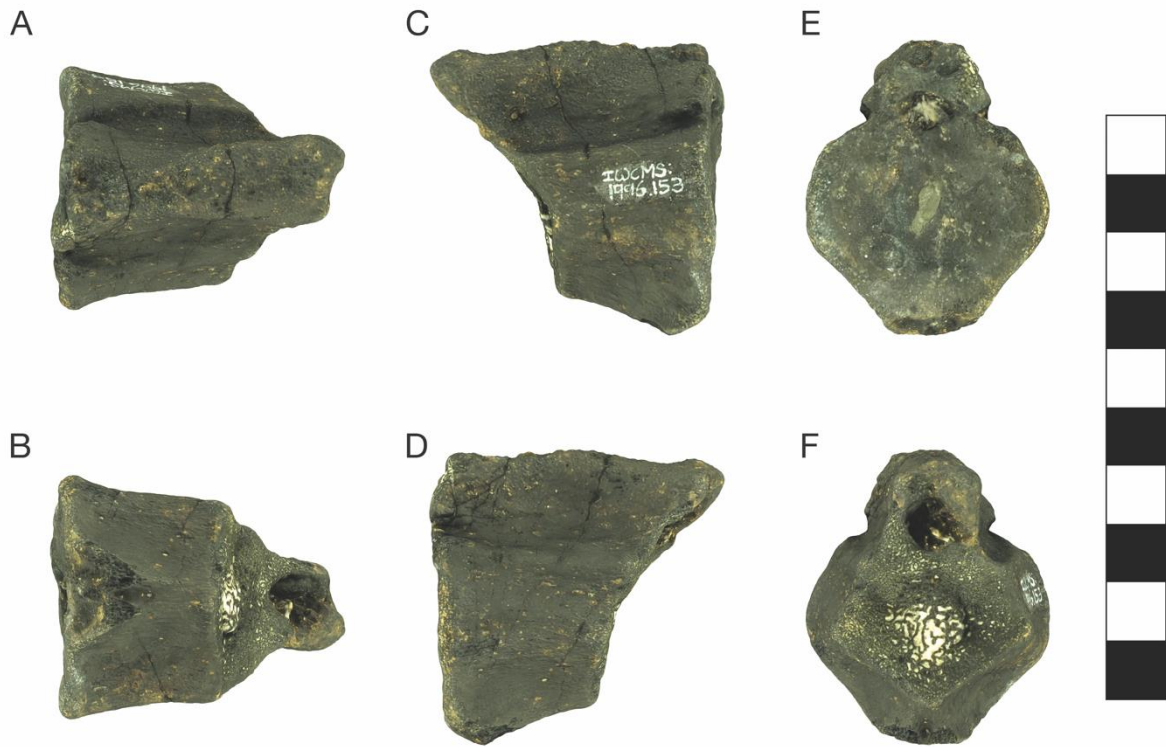


**Fig. S22. Caudal vertebra.** Orientation presumed: A, dorsal; B, ventral; C, left lateral; D, right lateral; E, anterior; F, posterior.

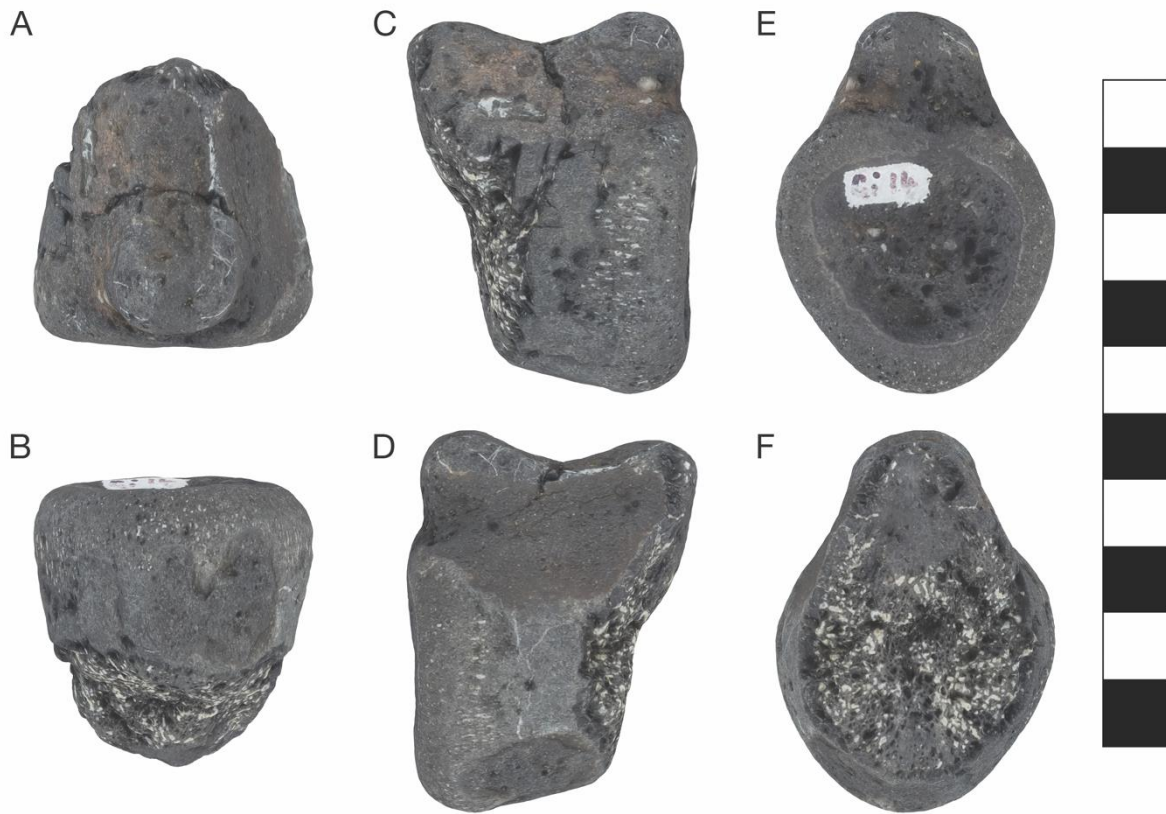


**Fig. S23. Caudal vertebra.** Orientation presumed: A, dorsal; B, ventral; C, left lateral; D, right lateral; E, anterior; F, posterior.

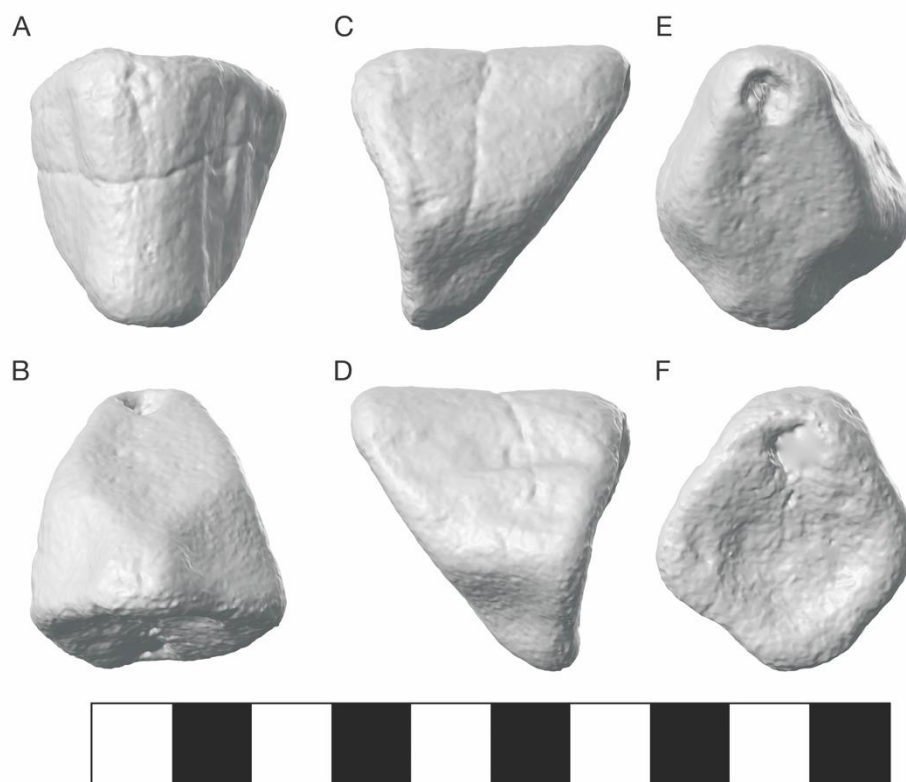
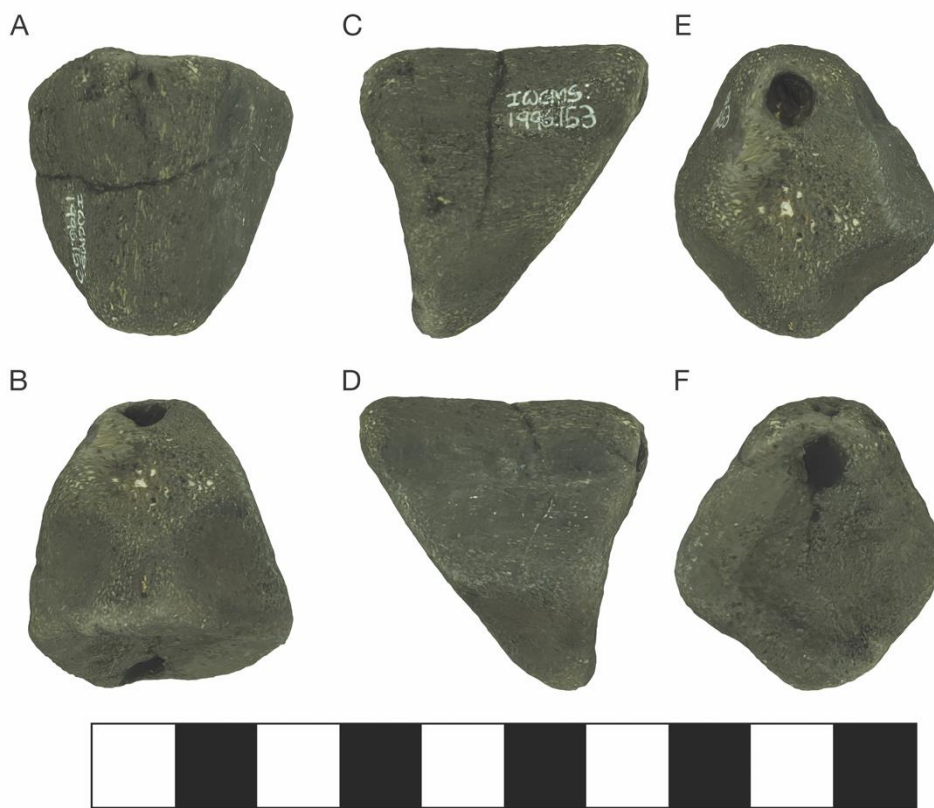


**Fig. S24. Caudal vertebra.** Orientation presumed: A, dorsal; B, ventral; C, left lateral; D, right lateral; E, anterior; F, posterior.



Fig. S25. Iliosacral block. A, dorsal; B, ventral; C, left lateral; D, right lateral; E, anterior; F, posterior.

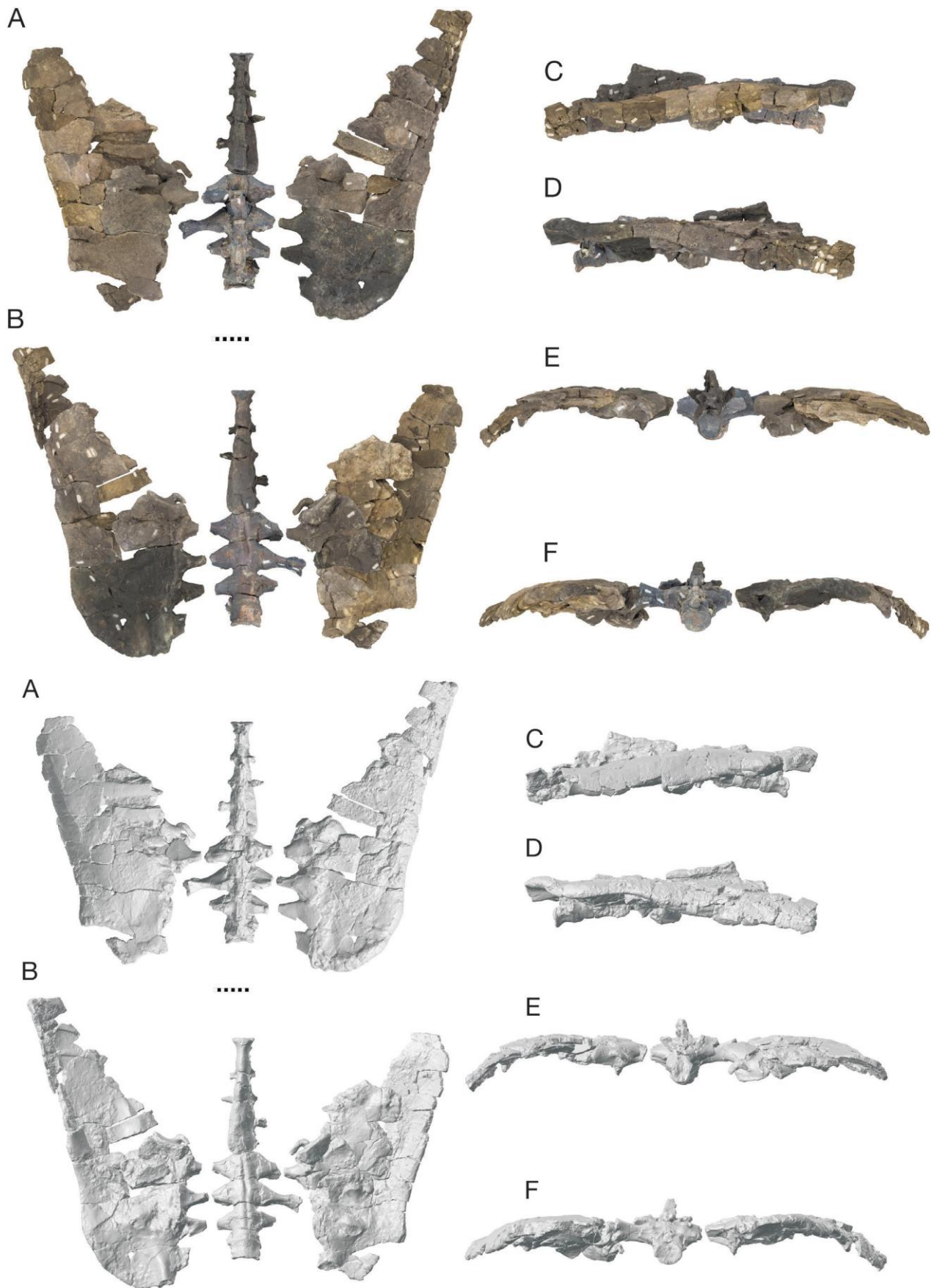


**Fig. S26. Left ischium.** A, proximal; B, distal; C, lateral; D, medial; E, anterior views; F, posterior.



**Fig. S27. Right ischium.** A, proximal; B, distal; C, lateral; D, medial; E, anterior; F, posterior.

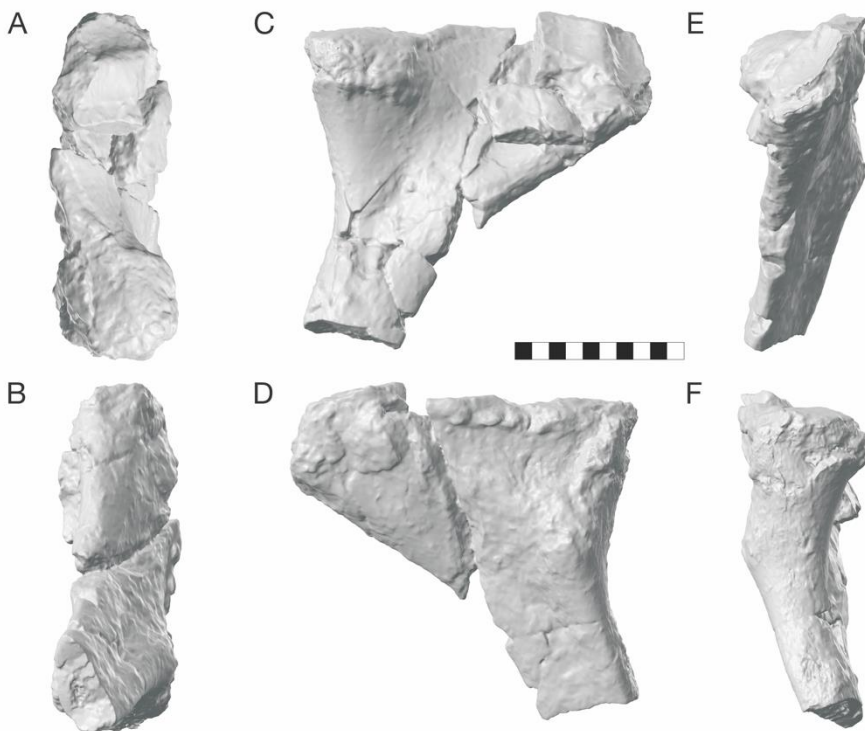


**Fig. S28. ?Fibula.** Presumed orientation: A, ?dorsal; B, ?ventral; C, ? lateral; D, ?medial; E, ?anterior; F, ?posterior.

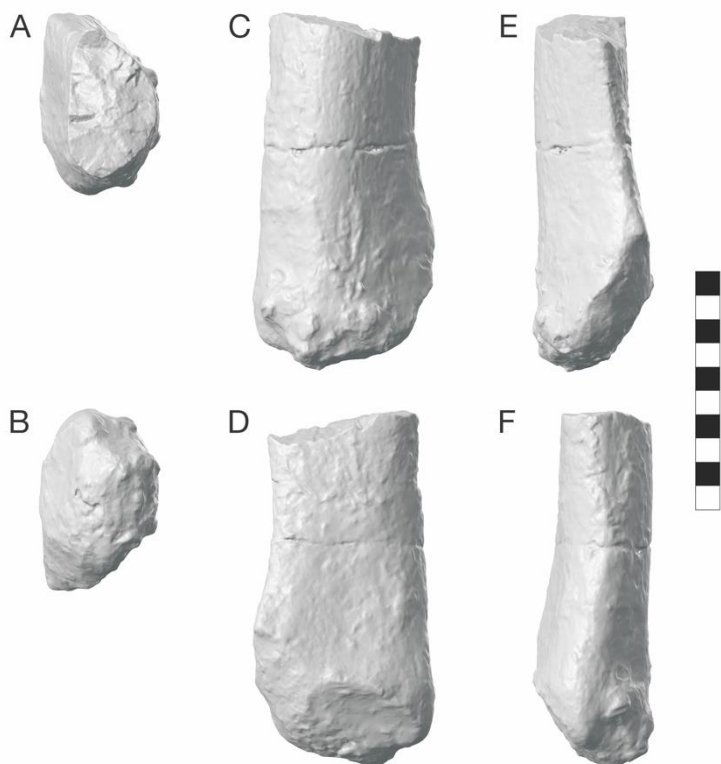


**Fig. S29. Flattened blade-like spine.** Orientation presumed: A, dorsal; B, ventral; C, proximal; D distal; E, anterior; F, posterior.

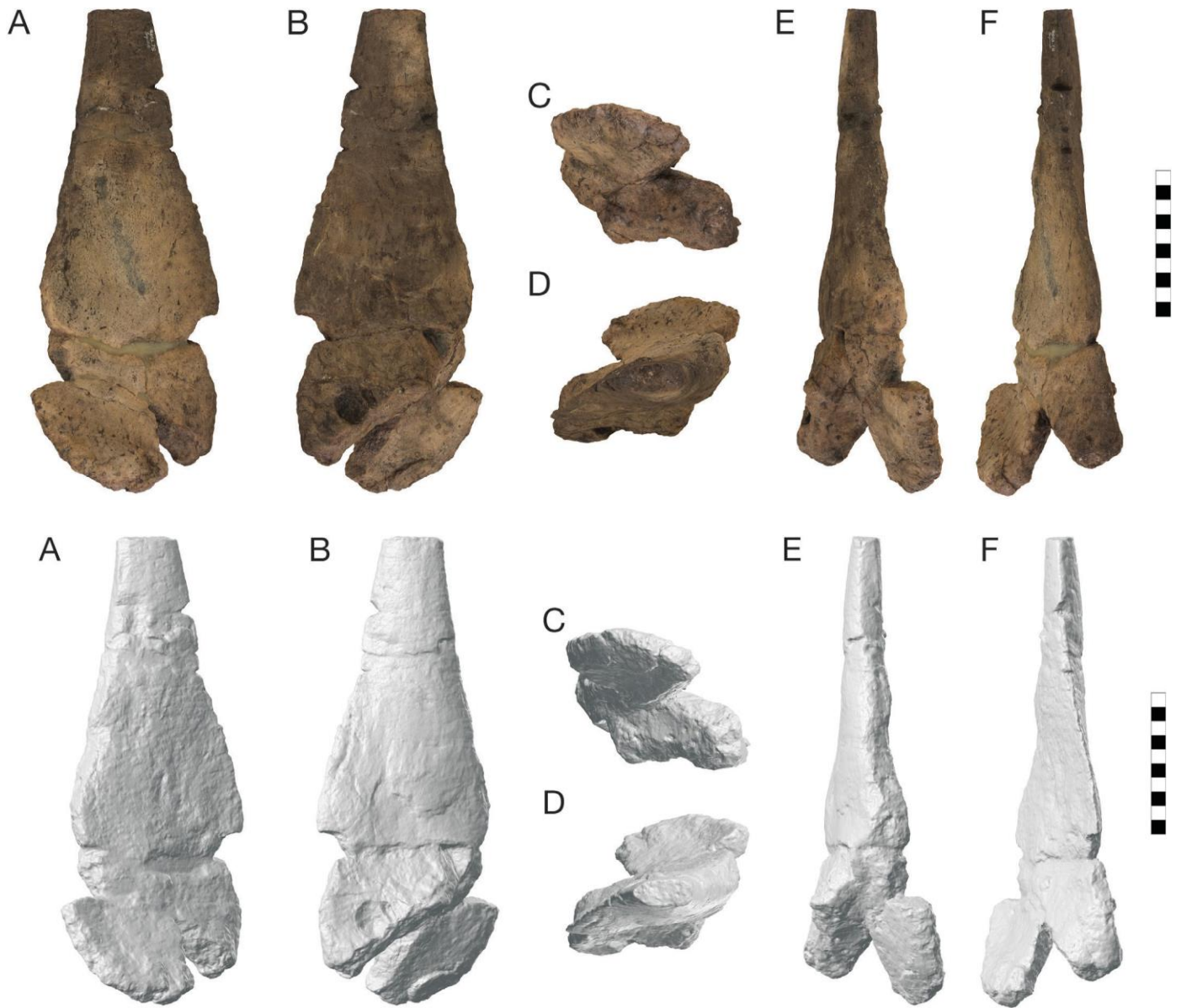


**Fig. S30. Flattened blade-like spine.** Orientation presumed: A, dorsal; B, ventral; C, proximal; D distal; E, anterior; F, posterior.

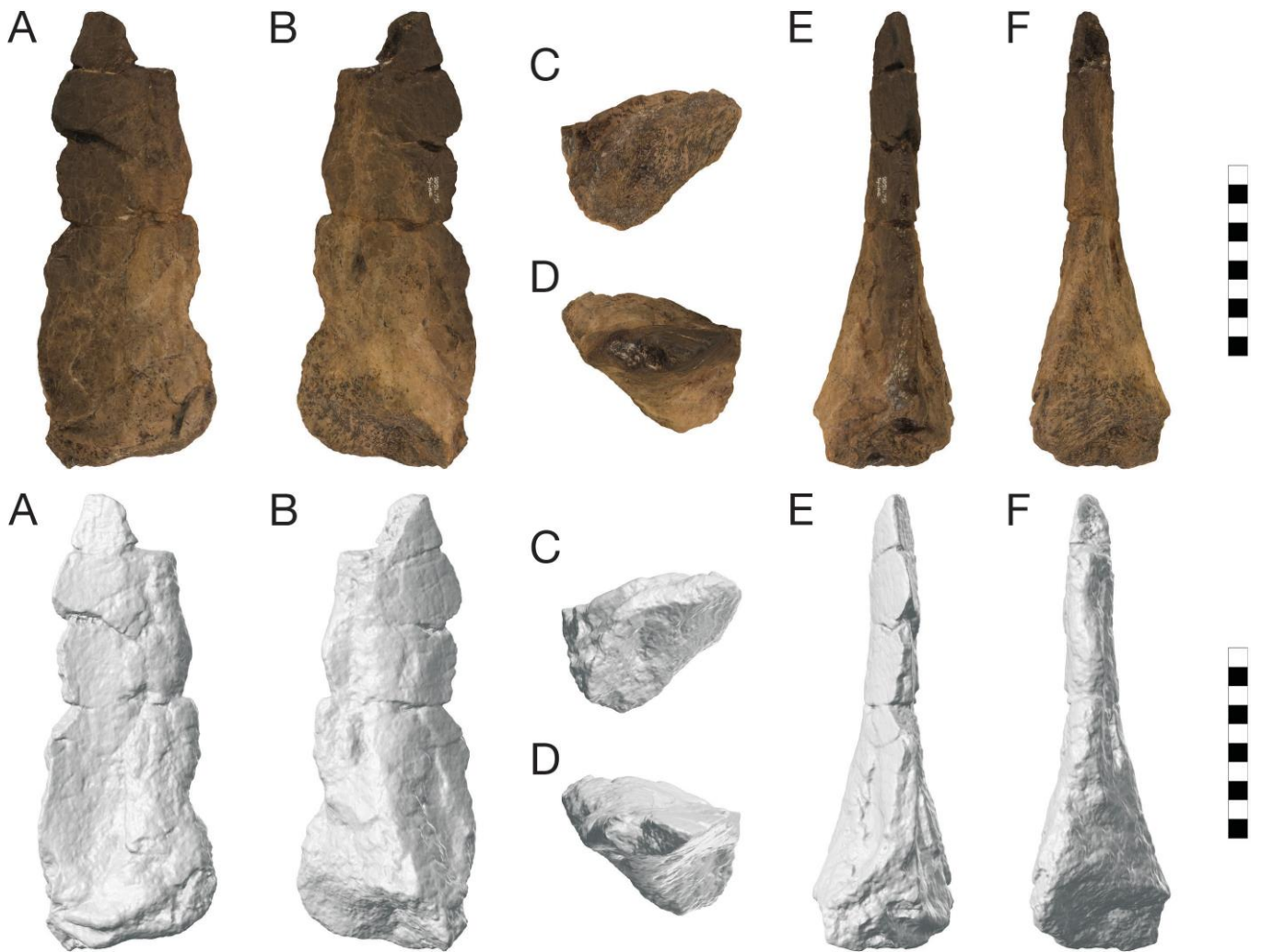
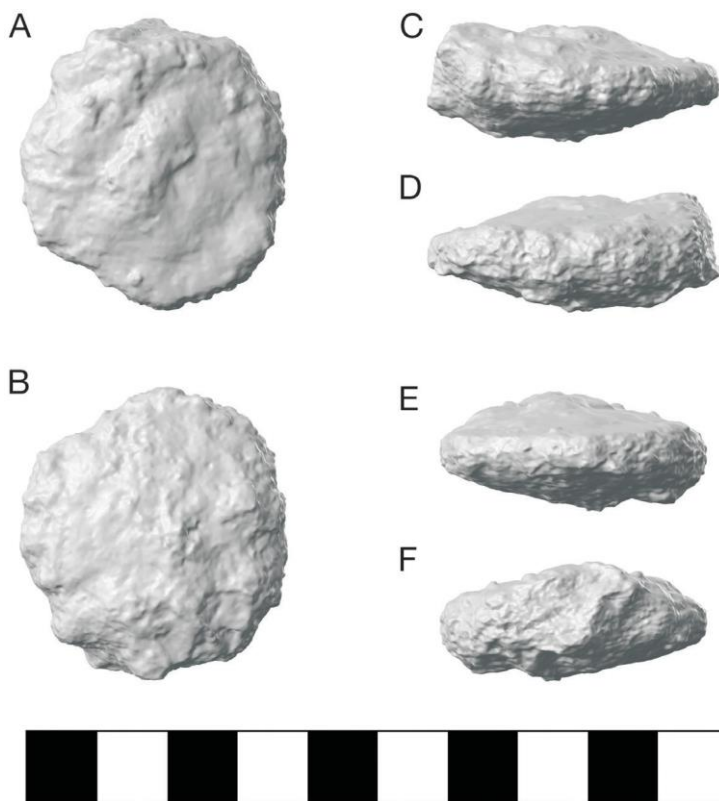
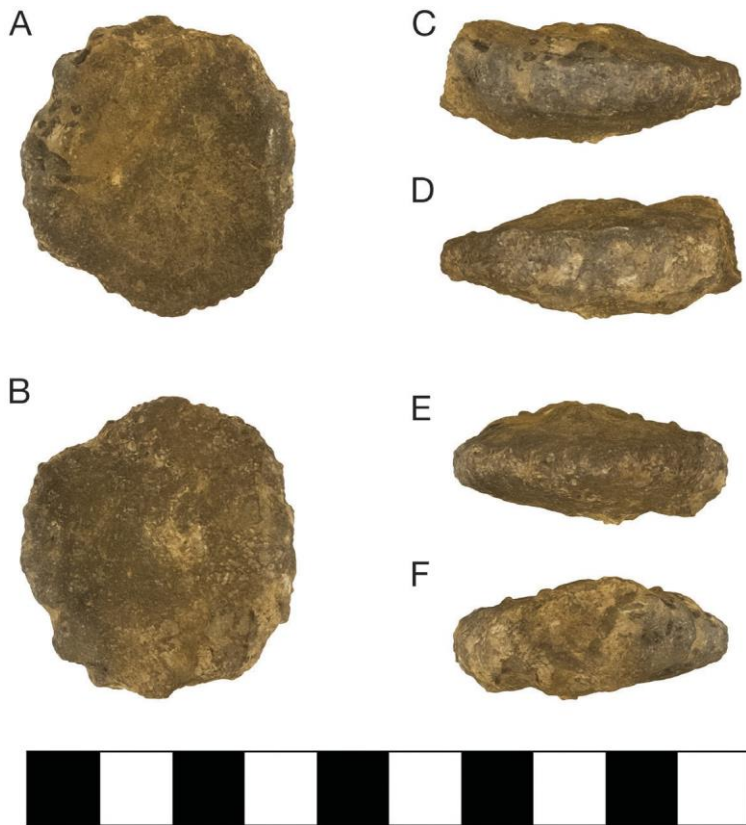


**Fig. S31. Small spine with unexpanded base.** Orientation presumed: A, distal; B, proximal; C, left lateral; D, right lateral; E, anterior; F, posterior.



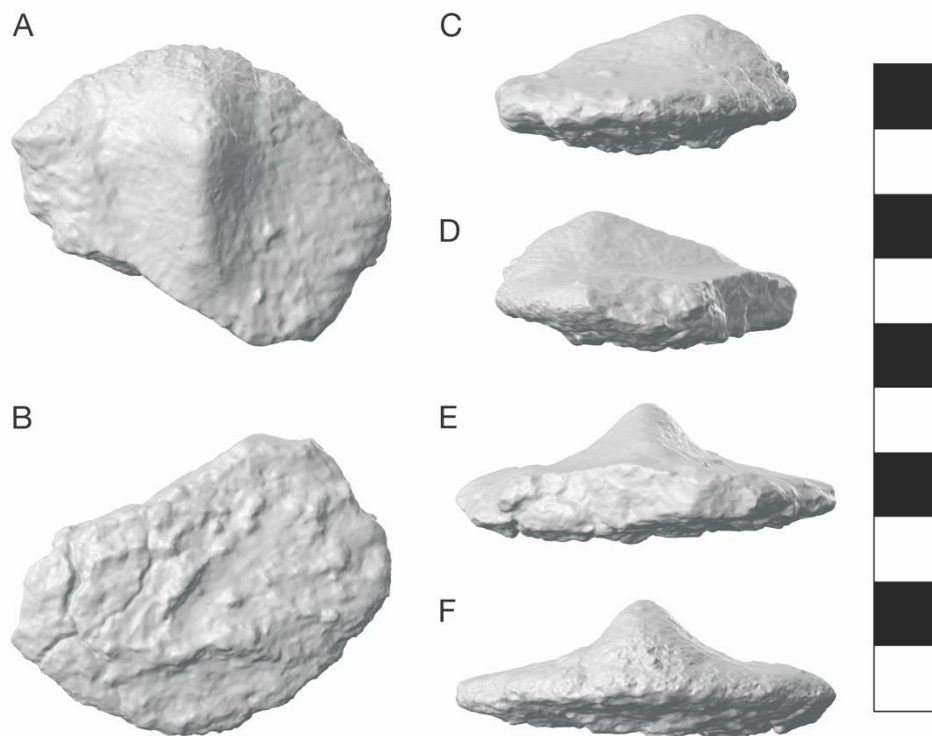
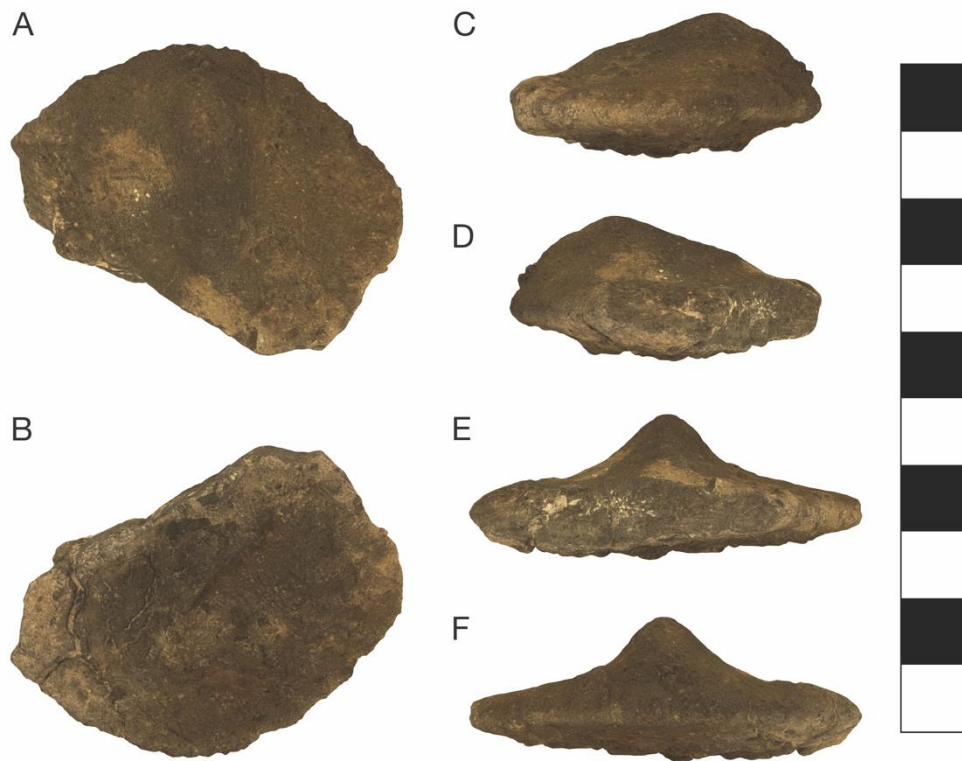
[Type here]

**Fig. S32. Small spine with unexpanded base.** Orientation presumed: A, dorsal; B, ventral; C, left lateral; D, right lateral; E, anterior; F, posterior



[Type here]

**Fig. S33. Small spine with unexpanded base.** Orientation presumed: A, dorsal; B, ventral; C, left lateral; D, right lateral; E, anterior; F, posterior



[Type here]

## References:

Brusatte, S.L. *Dinosaur Paleobiology*. John Wiley and Sons, Ltd. (2018)

Coombs Jr., W. P. Osteology and myology of the hindlimb in the Ankylosauria (Reptilia, Ornithischia). *J. Paleontol.* **53**, 666–684 (1979)

Díez Díaz, V., Mallison, H., Asbach, P., Schwarz, D. & Blanco, A. Comparing surface digitization techniques in palaeontology using visual perceptual metrics and distance computations between 3D meshes. *Palaeontology* 1–24 (2021). doi:10.1111/pala.12518

Fahlke, J. M. & Autenrieth, M. Photogrammetry Vs. Micro-Ct Scanning for 3D Surface Generation of a Typical Vertebrate Fossil - A Case Study. *J. Paleontol. Tech.* **14**, 1–18 (2016).

Sellers W.I, Pond S.B. 2015. Kinect controlled dinosaur simulations for education and public outreach. PeerJ PrePrints 3:e1584v1 <https://doi.org/10.7287/peerj.preprints.1584v1>

Senter, P. Evidence for a sauropod-like metacarpal configuration in stegosaurian dinosaurs. *Acta Palaeontol. Pol.* **55**, 427–432 (2010).

Shelburne, E. C. H. & Thompson, A. C. Specimen whitening: an assessment of methods of ammonium chloride smoke removal. *Collect. Forum* **30**, 63–72 (2016).

Witmer, L. M. & Ridgely, R. C. The paranasal air sinuses of predatory and armored dinosaurs (Archosauria: Theropoda and ankylosauria) and their contribution to cephalic structure. *Anat. Rec.* **291**, 1362–1388 (2008).

Witton, M. P. (2018). *Palaeoartist's Handbook: Recreating Prehistoric Animals in Art*. Ramsbury: The Crowood Press.